1974-09

Available potential energy in numerical ocean circulation models

Alcorn, Marion Everet

Monterey, California. Naval Postgraduate School

AVAILABLE POTENTIAL ENERGY IN NUMERICAL OCEAN CIRCULATION MODELS

Marion Everet Alcorn

NAVAL POSTGRADUATE SCHOOL
Monterey, California

THESIS

AVAILABLE POTENTIAL ENERGY IN
NUMERICAL OCEAN CIRCULATION MODELS

by

Marion Everet Alcorn

September 1974

Thesis Advisor: R.L.Haney

SECURITY CLASSIFICATION OF THIS PAGE (When Data Entered)

REPORT DOCUMENTATION PAGE

READ INSTRUCTIONS BEFORE COMPLETING FORM

1. REPORT NUMBER	2. GOVT ACCESSION NO. / 3. RECIPIENT'S CATALOG NUMBER
4. TITLE (and Subtitle): Available Potential Energy in Numerical Ocean Circulation Models	5. TYPE OF REPORT & PERIOD COVERED: Master's Thesis, September 1974
	6. PERFORMING ORG. REPORT NUMBER
7. AUTHOR(s): Marion Everet Alcorn	8. CONTRACT OR GRANT NUMBER(s)
9. PERFORMING ORGANIZATION NAME AND ADDRESS: Naval Postgraduate School, Monterey, California 93940	10. PROGRAM ELEMENT, PROJECT, TASK AREA & WORK UNIT NUMBERS
11. CONTROLLING OFFICE NAME AND ADDRESS: Naval Postgraduate School, Monterey, California 93940	12. REPORT DATE: September 1974
	13. NUMBER OF PAGES: 66
14. MONITORING AGENCY NAME & ADDRESS (if different from Controlling Office)	15. SECURITY CLASS. (of this report): Unclassified
	15a. DECLASSIFICATION/DOWNGRADING SCHEDULE

16. DISTRIBUTION STATEMENT (of this Report)

Approved for public release; distribution unlimited.

17. DISTRIBUTION STATEMENT (of the abstract entered in Block 20, if different from Report)

18. SUPPLEMENTARY NOTES

19. KEY WORDS (Continue on reverse side if necessary and identify by block number)

Available Potential Energy
Numerical Ocean Circulation Models
MODE eddies

20. ABSTRACT (Continue on reverse side if necessary and identify by block number)

The energetics of two numerical models of the ocean circulation are studied by use of available potential energy. Available potential energy, calculated by an approximation equation using a temperature perturbation field, compares favorably with that obtained using the exact expression using a height perturbation field.

A general circulation model of the ocean is employed to

DD FORM 1 JAN 73 1473 EDITION OF 1 NOV 65 IS OBSOLETE
S/N 0102-014-6601 |
(Page 1)

SECURITY CLASSIFICATION OF THIS PAGE (When Data Entered)

study large-scale energy transformations, and a mid-ocean dynamics experiment (mesoscale) model is employed to study transformations of energy by stationary features and by transient motions. Results from the general circulation model are consistent with those of Haney (1974). Results from the mesoscale model indicate that the transformation of energy is from available potential energy to kinetic energy of the transient eddy field.

Available Potential Energy

in

Numerical Ocean Circulation Models

by

Marion Everet Alcorn
Lieutenant Junior Grade United States Naval Reserve
B.S., Fort Hays Kansas State College, 1968

Submitted in partial fulfillment of the
requirements for the degree of

MASTER OF SCIENCE IN METEOROLOGY

from the

U.S. NAVAL POSTGRADUATE SCHOOL

September 1974

ABSTRACT

The energetics of two numerical models of the ocean circulation are studied by use of available potential energy. Available potential energy, calculated by an approximation equation using a temperature perturbation field, compares favorably with that obtained using the exact expression using a height perturbation field.

A general circulation model of the ocean is employed to study large-scale energy transformations, and a mid-ocean dynamics experiment (mesoscale) model is employed to study transformations of energy by stationary features and by transient motions. Results from the general circulation model are consistent with those of Haney (1974). Results from the mesoscale model indicate that the transformation of energy is from available potential energy to kinetic energy of the transient eddy field.

TABLE OF CONTENTS

LIST OF FIGURES

ACKNOWLEDGEMENT

The author wishes to take this opportunity to express his appreciation for the guidance and assistance offered by his advisor, Professor R.L. Haney, throughout this research and during the author's tenure at the Naval Postgraduate School.

Sincerest thanks are also extended to Professor R.L. Elsberry, who acted as second reader for this thesis, and to the professors and staff of the Meteorology Department for their excellent instruction and advice.

The author also desires to acknowledge the patience and understanding of his wife, Jacqulin, through two years of graduate study.

I. INTRODUCTION

A basic part of any study of an atmospheric or oceanic circulation system is a study of the behavior of the energy in the system and its transformation from one form of energy to another. The various forms of energy can be separated into three basic forms of energy: kinetic energy, potential energy and internal energy. Haurwitz (1941) showed that the potential energy and internal energy, in a vertical column, are proportional under hydrostatic equilibrium and thus may be combined into a single parameter, the total potential energy. Conversions of energy then occur between total potential energy and kinetic energy.

A. AVAILABLE POTENTIAL ENERGY IN ATMOSPHERIC CIRCULATION

Lorenz (1955), in a study of atmospheric circulation, showed that since total potential energy was three to four orders of magnitude larger than kinetic energy, transformation of energy between the two energy forms was difficult to study. In a horizontally stratified atmosphere, heating of the atmosphere disturbs the stratification, allowing potential energy to be converted to kinetic energy. However, cooling of the atmosphere, which removes total potential energy from the system, also disturbs the stratification and creates conditions for conversion of total potential energy to kinetic energy.

Lorenz (1955) defined available potential energy as the difference between the total potential energy of the whole atmosphere and the total potential energy that would exist if the mass of the atmosphere were redistributed with conservation of potential temperature to form a horizontally stable atmosphere. Then, under adiabatic flow, the sum of the available potential energy and kinetic energy is conserved.

B. AVAILABLE POTENTIAL ENERGY IN OCEANIC CIRCULATION

The use of the concept of available potential energy can be carried into the study of oceanic circulations. Several studies of the energetics of the ocean circulation systems have been based on available potential energy, as in Barrett (1971), and Wright (1972). The study by Wright dealt with changes in available potential energy in the ocean general circulation. The cooling of cold, high latitude water and the surface warming of warm equatorial water produces available potential energy by increasing the stratification of the ocean mass. Conversely, the sinking of the cold surface water in the north tends to convert available potential energy to kinetic energy as it returns the water mass to a more stably stratified system. Barrett (1971) studied the available potential energy in the transient motion of Gulf Stream rings. Results of the study indicated that the decay of cold-core rings in the western Sargasso Sea region reduced the available potential energy of the

region. The presence of decaying cold-core rings in the western Sargasso Sea should have resulted in a rising of the mean thermocline in that region. Since the thermocline was not observed to rise significantly in the western Sargasso Sea region, a local energy source must have been present to counteract the energy loss.

C. AVAILABLE POTENTIAL ENERGY IN NUMERICAL OCEAN CIRCULATION MODELS

This study applied available potential energy calculations to two experiments with a numerical model of the ocean general circulation; one simulating large-scale, quasi-steady state motion and the other simulating mesoscale transient motion. It was desired to calculate available potential energy using a perturbation height field compared with an approximate calculation using a temperature perturbation field. An expression for the balance of available potential energy was obtained from this approximation equation. The importance of the terms in the expression for the balance of available potential energy, and their corresponding physical processes, could then be examined in the two numerical experiments.

II. DESCRIPTION OF THE NUMERICAL MODELS

The first experiment utilized the general circulation model of the ocean, as described in part A, for large-scale quasi-steady state motion. The Mid-Ocean Dynamics Experiment model (Robinson, et.al., 1974, MODE, Hot Line News, No. 57.), as described in part B, was utilized for the transient motion experiment.

A. GENERAL CIRCULATION MODEL OF THE OCEAN

The model represents an idealized ocean basin with a flat bottom and regular coast. It is everywhere 4 km deep, 90° longitude wide and extends from 51.25S to 48.75N. The grid intervals are 3° of longitude and 2.5° of latitude. There are six vertical levels, placed at 20, 100, 300, 700, 1500, 3000 meters below the undisturbed surface. The model is based on the primitive equations which are integrated in time from specified initial conditions. The equations are based on the hydrostatic and Boussinesq approximations. The ocean is thus assumed incompressible. Salinity is neglected and density is a linear function of temperature. The equations are

$$\frac{du}{dt} = \frac{-1}{\rho_o a\cos\varphi}\frac{\partial p}{\partial \lambda} + fv + \frac{u}{a\cos\varphi}v\sin\varphi + A_m\nabla^2 u + K\frac{\partial^2 u}{\partial z^2}, \quad (1)$$

$$\frac{dv}{dt} = \frac{-1}{\rho_0 a}\frac{\partial p}{\partial \varphi} - fu - \frac{u}{a\cos\varphi}u\sin\varphi + A_M\nabla^2 v + K\frac{\partial^2 v}{\partial z^2} \qquad (2)$$

$$\frac{\partial p}{\partial z} = -\rho g \qquad (3)$$

$$\frac{\partial w}{\partial z} + \frac{1}{a\cos\varphi}\left[\frac{\partial u}{\partial \lambda} + \frac{\partial (v\cos\varphi)}{\partial \varphi}\right] = 0 \qquad (4)$$

$$\frac{dT}{dt} = A_H\nabla^2 T + K\frac{\partial^2 T}{\partial z^2} + \delta(T) \qquad (5)$$

$$\rho = \rho_0\left(1 - \alpha(T - T_0)\right), \qquad (6)$$

where the symbols have the following meanings:

t = time

λ = longitude

φ = latitude

Z = height

Ω = angular speed of earth's rotation

f = coriolis force ($=2\Omega\sin\varphi$)

a = radius of earth

g = acceleration of gravity

u = eastward velocity component

v = northward velocity component

w = vertical velocity component

T = temperature

T_0 = constant reference temperature

ρ = density

ρ_o = density of water at reference temperature

α = coefficient of thermal expansion

H = depth of ocean basin

$\delta_c(T)$ = convective adjustment of T if lapse rate becomes unstable.

The lateral boundary conditions on heat and momentum at all four walls of the basin are those of perfect insulation and zero slip. The ocean floor is thermally insulated, but free slip is allowed. Due to the flat bottom, the vertical velocity is zero there. The circulation is driven and controlled by the wind stress and heat flux at the ocean surface. The wind stress is larger in the southern hemisphere and meridional wind stress is neglected. The net downward heat flux at the ocean surface is expressed as

$$Q = Q_2(T_a^* - T_s),$$

where T_s is the ocean surface temperature, T_a^* is an atmospheric equilibrium temperature approximately equal to the air temperature at 10 meters and Q_2 is a coupling coefficient determined from atmospheric climatological data. In this model, T_s is the temperature at the top level, 20 meters below the surface. The model is a coarse-grid, high-viscosity model designed to show large scale ocean circulation. Complete documentation of the model is given in Haney (1974).

B. MID-OCEAN DYNAMICS EXPERIMENT MODEL

The mid-ocean dynamics experiment, MODE, model is a modification of the previously described model. It is designed to resolve mesoscale eddies with a horizontal grid resolution of 40 km and 5 levels in the vertical. A 2000 km square section of the general circulation model area is represented by the MODE model, located along the western boundary and centered at 35N. Circulation is driven and controlled by the wind stress and thermal forcing, the same as in the previous model, but the eddy viscosity and conductivity were reduced to achieve mesoscale eddies. Eastern and western boundaries are thermally insulated, no-slip walls, as in the general circulation model. Northern and southern boundary conditions are taken as free slip, zero normal velocity and a vertical temperature distribution which is independent of longitude and time. The ocean floor is thermally insulated as in the general circulation model. Initial conditions for the model were zero velocity and a temperature of 5^{0}C at all levels. Twenty years of integration was performed on a 100 km X 100 km grid using a horizontal viscosity of $A_m = 2 \times 10^7$ cm^2/sec and heat diffusivity of $A_H = 1 \times 10^7$ cm^2/sec. Ten years of fine grid calculations were then made using $A_m = 2 \times 10^6$ cm^2/sec and $A_H = 5 \times 10^6$ cm^2/sec.

III. DERIVATION OF AVAILABLE POTENTIAL ENERGY EQUATIONS

A. DOMAIN AVERAGED AVAILABLE POTENTIAL ENERGY

The vertically averaged available potential energy contained within an idealized ocean basin may be calculated as follows. Assume the basin to be flat bottomed at a depth H. The total potential energy per unit volume in a column in the basin is given as

$$P = \frac{1}{H}\int_{-H}^{0} \rho g z \, dz \,,$$

where Z increases upward from the bottom where Z = -H. All variations in H are neglected. Neglecting also the dependence of density on pressure and salinity, the density may be written as a linear function of temperature, equation (6). The total potential energy per unit volume in the column is then given as

$$P = \text{CONSTANT} - \frac{g\alpha\rho_0}{H}\left[\int_{z=-H}^{z=0} d\left(\frac{TZ^2}{2}\right) - \int_{T(-H)}^{T(0)} \frac{Z^2}{2}\, dT\right].$$

By defining Z(T) = 0 if $T \geq T(0)$ and Z(T) = -H if $T \leq T(-H)$, the vertical average total potential energy per unit volume in the column may be written as

$$P = \text{CONSTANT} - \frac{g\alpha\rho_0}{H}\,\frac{T(-H)}{2}\,H^2 + \frac{g\alpha\rho_0}{H}\int_{T_{min}}^{T_{MAX}} \frac{Z^2}{2}\, dT \,,$$

where Tmin and Tmax represent the coldest and warmest temperatures found in the basin respectively. The vertical average total potential energy averaged over the horizontal domain, denoted by $(\bar{\ })$, is given by

$$\bar{P} = \text{CONSTANT} - \frac{g\alpha\rho_0}{H}\frac{\bar{T}(-H)H^2}{2} + \frac{g\alpha\rho_0}{H}\int_{T_{MIN}}^{T_{MAX}} \frac{\overline{Z^2}}{2}\,dT,$$

where the bar over Z^2 denotes an average over an isothermal surface. The average potential energy is a minimum when $\overline{Z^2}$ is a minimum, ie. Z is equal to $\bar{Z}$ everywhere. Writing the height of a temperature surface as a mean height, $\bar{Z}$, and a departure from the mean, Z', then the domain average total potential energy is a minimum when Z' is zero everywhere. In this case, $\overline{Z^2}$ can be replaced by $\bar{Z}^2$. The minimum domain averaged total potential energy can then be written as

$$\bar{P}_{MIN} = \text{CONSTANT} - \frac{g\alpha\rho_0}{H}\frac{\bar{T}(-H)_{MIN}H^2}{2} + \frac{g\alpha\rho_0}{H}\int_{T_{MIN}}^{T_{MAX}} \frac{\bar{\bar{Z}}^2}{2}\,dT.$$

If the difference between the average bottom temperature, $\bar{T}(-H)$, and the average bottom temperature in the state of minimum domain averaged total potential energy, $\bar{T}(-H)\text{min}$, is assumed small and thus can be neglected, then the domain average available potential energy can be written as

$$\bar{A} = \frac{g\alpha\rho_0}{H}\int_{T_{MIN}}^{T_{MAX}} \frac{1}{2}\left(\overline{Z^2} - \bar{Z}^2\right)dT,$$

which can be written as

$$\bar{A} = \frac{g\alpha\rho_0}{H}\int_{T_{MIN}}^{T_{MAX}} \frac{1}{2}\overline{Z'^2}\,dT. \qquad (7)$$

Thus, the available potential energy is proportional to the variance of height of an isothermal surface.

B. APPROXIMATION TO THE DOMAIN AVERAGE AVAILABLE POTENTIAL ENERGY

The variance of height over an isothermal surface, $\overline{Z'^2}$, can be related to the variance of temperature over a horizontal surface, assuming the ocean is stably stratified. When the perturbation, Z', from the mean height of an isothermal surface is greater than zero, the temperature of this region is less than the mean temperature by an amount T'. Similarly, when Z' is less than zero, T' is greater than zero. Therefore, changes due to Z' are partially compensated by changes in T'. The height of a temperature surface may be approximated by

$$Z(T) \approx \bar{Z}(\bar{T}) = \bar{Z}(T-T'),$$

which shows the height perturbation can be approximated by

$$Z'(T) \approx T' \frac{\partial \bar{Z}}{\partial T} .$$

When this is substituted into the expression for the domain average available potential energy, equation (7), the approximation to the domain average available potential energy is then

$$\bar{A} = \frac{g\alpha\rho_0}{H} \int_{T_{min}}^{T_{MAX}} \frac{1}{2} \left(T' \frac{d\bar{Z}}{dT} \right)^2 dT ,$$

which can be written as

$$\bar{A} = \frac{g\alpha\rho_0}{H} \int_{-H}^{0} \frac{\overline{\frac{1}{2} T'^2}}{\frac{\partial \bar{T}}{\partial Z}} dz . \qquad (8)$$

C. THE BALANCE OF AVAILABLE POTENTIAL ENERGY

Since available potential energy is a very important source for kinetic energy, a study of the energetics of an ocean circulation should include a study of production and dissipation of available potential energy. Under adiabatic conditions an increase in kinetic energy is compensated by a decrease of available potential energy. When both energy forms increase, then formation of available potential energy must be occurring through diabatic processes. A study of these generation and dissipation processes and their importance may be made through use of the equation of the balance of available potential energy. The equation is derived as follows, based on the approximate form (8) of available potential energy.

From equation (8), the time rate of change of available potential energy is

$$\frac{\partial \bar{A}}{\partial t} = \frac{g\alpha\rho_0}{H}\left[\int_{-H}^{0} \frac{1}{\left(\frac{\partial \bar{T}}{\partial z}\right)} \frac{\partial}{\partial t}\left(\overline{\frac{1}{2}T'^2}\right) dz - \int_{-H}^{0} \frac{\overline{\frac{1}{2}T'^2}}{\left(\frac{\partial \bar{T}}{\partial z}\right)^2} \frac{\partial}{\partial t}\left(\frac{\partial \bar{T}}{\partial z}\right) dz\right]. \quad (9)$$

By use of the thermodynamic equation (5), equation (9) was rewritten to show the various terms responsible for the change of available potential energy. The term $\frac{\partial}{\partial t}\left(\overline{\frac{1}{2}T'^2}\right)$ can be written as

$$\frac{\partial}{\partial t}\left(\overline{\frac{1}{2}T'^2}\right) = \overline{T'\frac{\partial T'}{\partial t}}. \quad (10)$$

The term $\frac{\partial}{\partial t}\left(\frac{\partial \bar{T}}{\partial z}\right)$ can be written as

$$\frac{\partial}{\partial t}\left(\frac{\partial \bar{T}}{\partial z}\right) = \frac{\partial}{\partial z}\left(\frac{\partial \bar{T}}{\partial t}\right). \quad (11)$$

The local rate of change of temperature and its average were obtained from the thermodynamic equation

$$\frac{\partial T}{\partial t} = -\nabla\cdot(\mathbb{V}T) - \frac{\partial(wT)}{\partial z} + A_H\nabla^2 T + K\frac{\partial^2 T}{\partial z^2} + \delta_c(T). \qquad (12)$$

The horizontal average of (12) gave

$$\frac{\partial \bar{T}}{\partial z} = -\frac{\partial \overline{(wT)}}{\partial z} + K\frac{\partial^2 \bar{T}}{\partial z^2} + \overline{\delta_c(T)}, \qquad (13)$$

where the terms $\overline{-\nabla\cdot(\mathbb{V}T)}$ and $A_H\nabla^2 T$ were zero since advection and diffusion of heat vanish at the boundaries of the domain. Equation (11) was then written using (13) as

$$\frac{\partial}{\partial t}\left(\frac{\partial \bar{T}}{\partial z}\right) = \frac{\partial}{\partial z}\left[-\frac{\partial \overline{(wT)}}{\partial z} + K\overline{\frac{\partial^2 T}{\partial z^2}} + \overline{\delta_c(T)}\right], \qquad (14)$$

which can be rewritten as

$$\frac{\partial}{\partial t}\left(\frac{\partial \bar{T}}{\partial z}\right) = \frac{\partial}{\partial z}\left[-\frac{\partial \overline{(wT)}}{\partial z} + \overline{\frac{Q}{\rho_o c}}\right], \qquad (15)$$

where

$$\overline{\frac{Q}{\rho_o c}} = K\overline{\frac{\partial^2 T}{\partial z^2}} + \overline{\delta_c(T)}.$$

Equation (12) was written in terms of an average temperature and the departure from the average. Equation (13) was then subtracted from the result giving

$$\frac{\partial T'}{\partial t} = -\nabla\cdot(\mathbb{V}\bar{T}) - \nabla\cdot(\mathbb{V}T') - \frac{\partial(w\bar{T})}{\partial z} - \frac{\partial(wT')}{\partial z} + \frac{\partial(\overline{wT})}{\partial z} + \left(K\frac{\partial^2 T}{\partial z^2}\right)' + \left(A_H\nabla^2 T\right)' + \delta_c(T)' \qquad (16)$$

Equation (16) was then substituted into the right hand side of equation (10) to give

$$\frac{\partial}{\partial t}\left(\frac{1}{2}\overline{T'^2}\right) = \overline{T'\left[-\nabla\cdot(\mathbf{v}\bar{T}) - \frac{\partial(w\bar{T})}{\partial z}\right]} + \overline{T'\left[-\nabla\cdot(\mathbf{v}T') - \frac{\partial(wT')}{\partial z}\right]} + \overline{T'\left[\left(K_H\frac{\partial^2 T}{\partial z^2}\right)' + \left(A_H\nabla^2 T\right)' + \delta_c(T)'\right]}, \quad (17)$$

since

$$\overline{T'\frac{\partial(wT)}{\partial z}} = 0.$$

The first term on the right side of (17) can be written as

$$\overline{T'\left[-\nabla\cdot(\mathbf{v}\bar{T}) - \frac{\partial(w\bar{T})}{\partial z}\right]} = -\overline{T'\mathbf{v}\cdot\nabla\bar{T}} - \overline{T'\bar{T}\nabla\cdot\mathbf{v}} - \overline{T'w\frac{\partial\bar{T}}{\partial z}} - \overline{T'\bar{T}\frac{\partial w}{\partial z}}.$$

The term $\overline{-T\mathbf{V}\cdot\nabla\bar{T}}$ is equal to zero because $\nabla\bar{T}$ is zero. By use of the continuity equation (4), the equation reduces to

$$\overline{T'\left[-\nabla\cdot(\mathbf{v}\bar{T}) - \frac{\partial(w\bar{T})}{\partial z}\right]} = -\overline{T'w\frac{\partial\bar{T}}{\partial z}}. \quad (18)$$

Also, the second term on the right side of equation (17) can be written as

$$\overline{T'\left[-\nabla\cdot(\mathbf{v}T') - \frac{\partial(wT')}{\partial z}\right]} = -\overline{\frac{\partial}{\partial z}\left(\frac{wT'^2}{2}\right)}. \quad (19)$$

The last term of equation (17) can be written using the definition of Q as

$$\overline{T'\left[\left(A_H\nabla^2 T\right)' + \left(K_H\frac{\partial^2 T}{\partial z^2}\right)' + \delta(T)'\right]} = \overline{\frac{T'Q'}{\rho_0 c}} \quad (20)$$

Substitution of equations (18), (19), (20) into equation (17) and using the resulting equation along with equation (15) results in the following form for equation (9), the balance of available potential energy

$$\frac{\partial A}{\partial t} = \frac{g\alpha\rho_0}{H}\left\{\int_{-H}^{0}\left[-\overline{T'W'} - \frac{1}{\left(\frac{\partial\bar{T}}{\partial z}\right)}\frac{\partial}{\partial z}\left(\frac{\overline{WT'^2}}{2}\right) + \frac{1}{\left(\frac{\partial\bar{T}}{\partial z}\right)}\frac{\overline{T'Q'}}{C_0 C}\right]dz\right.$$
$$\left. -\int_{-H}^{0}\frac{\frac{1}{2}\overline{T'^2}}{\left(\frac{\partial\bar{T}}{\partial z}\right)^2}\frac{\partial}{\partial z}\left[-\frac{\partial(\overline{WT})}{\partial z} + \frac{\bar{Q}}{C_0 C}\right]dz\right\}. \qquad (21)$$

The balance of available potential energy is due to five terms on the right side of equation (21). The first term is the transformation between available potential energy and kinetic energy due to the correlation between temperature and vertical velocity. The second term is a triple correlation term due to the convergence of the vertical transport of temperature perturbations. The third term is the generation of available potential energy due to a spatial correlation between heating and perturbation temperature. The last two terms represent the change of available potential energy due to a change in the mean static stability. Lorenz (1955) assumed the static stability was constant in time and also neglected the triple correlation term leaving only the first and third terms on the right side of equation (21). In the quasi geostrophic theory, the first and third terms are the only terms to appear in the balance of available potential energy. For the general circulation model, all five terms were studied and for the mid-ocean dynamics experiment model the first three terms were studied.

IV. FINITE DIFFERENCE EQUATIONS

The numerical program developed for calculations of available potential energy and the balance of available potential energy was designed for the general circulation model as developed by Haney (1974). Therefore, the space finite differencing scheme and the boundary conditions were the same as those of the general circulation model, Haney (1974). A staggered grid system was used for placement of the variables. Figure 1 shows the variable placement in the horizontal and figure 2 shows the variable placement in the vertical. Longitude positions are designated by the subscript i, latitude positions by the subscript j and vertical positions by k, increasing downward.

Horizontal averaging, denoted by $\bar{q}$ for some variable q_{ij} was done in the following manner. Since the lateral boundaries were located at integer i,j points, the mean value of a term to be averaged was calculated at the $i+\frac{1}{2}, j+\frac{1}{2}$ positions based on the terms value at, and the areas of, the grid points at the four surrounding i,j positions. These mean values were then summed with equal weights to determine the domain horizontal average.

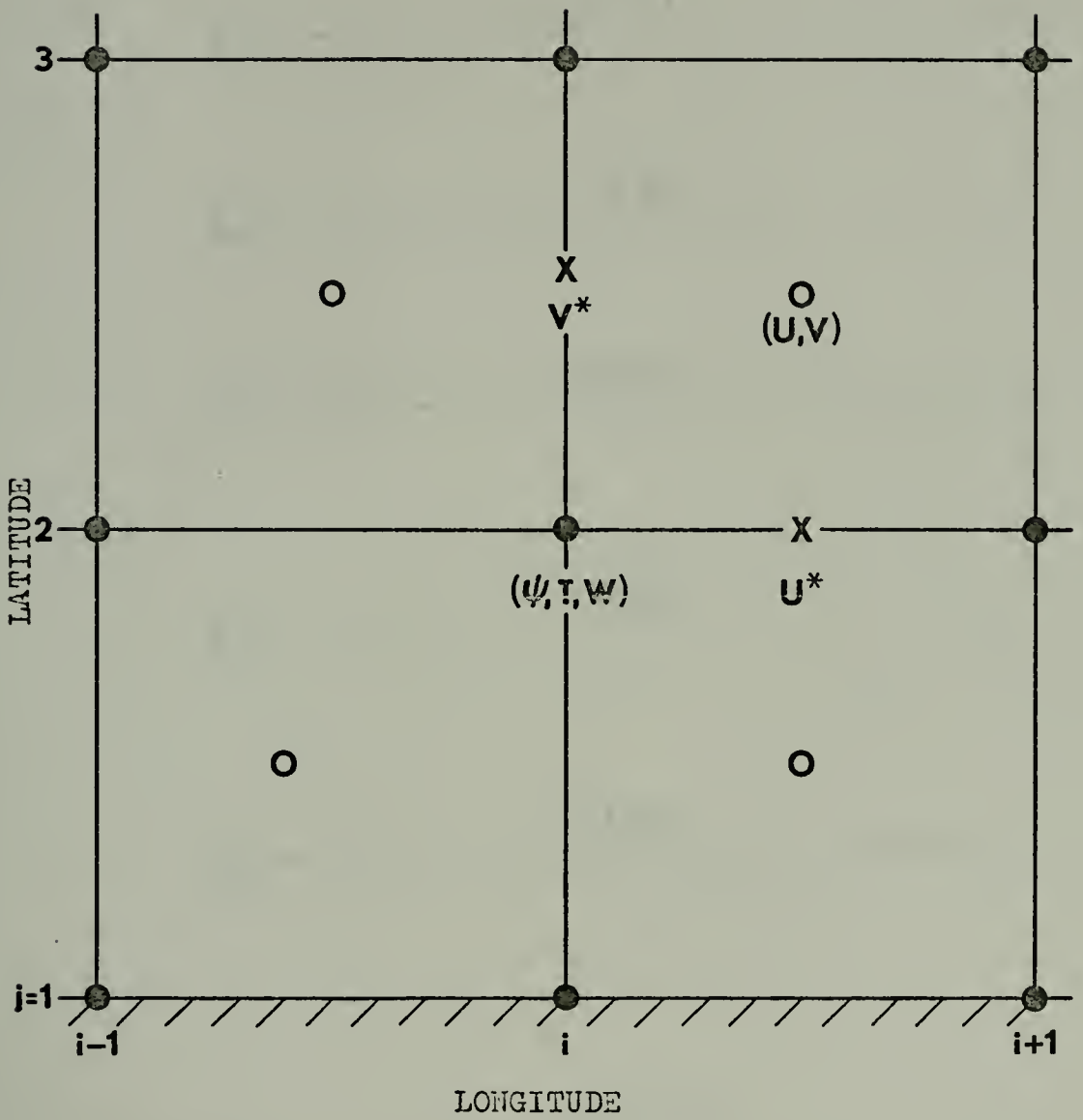

Figure 1. Horizontal Placement of Variables

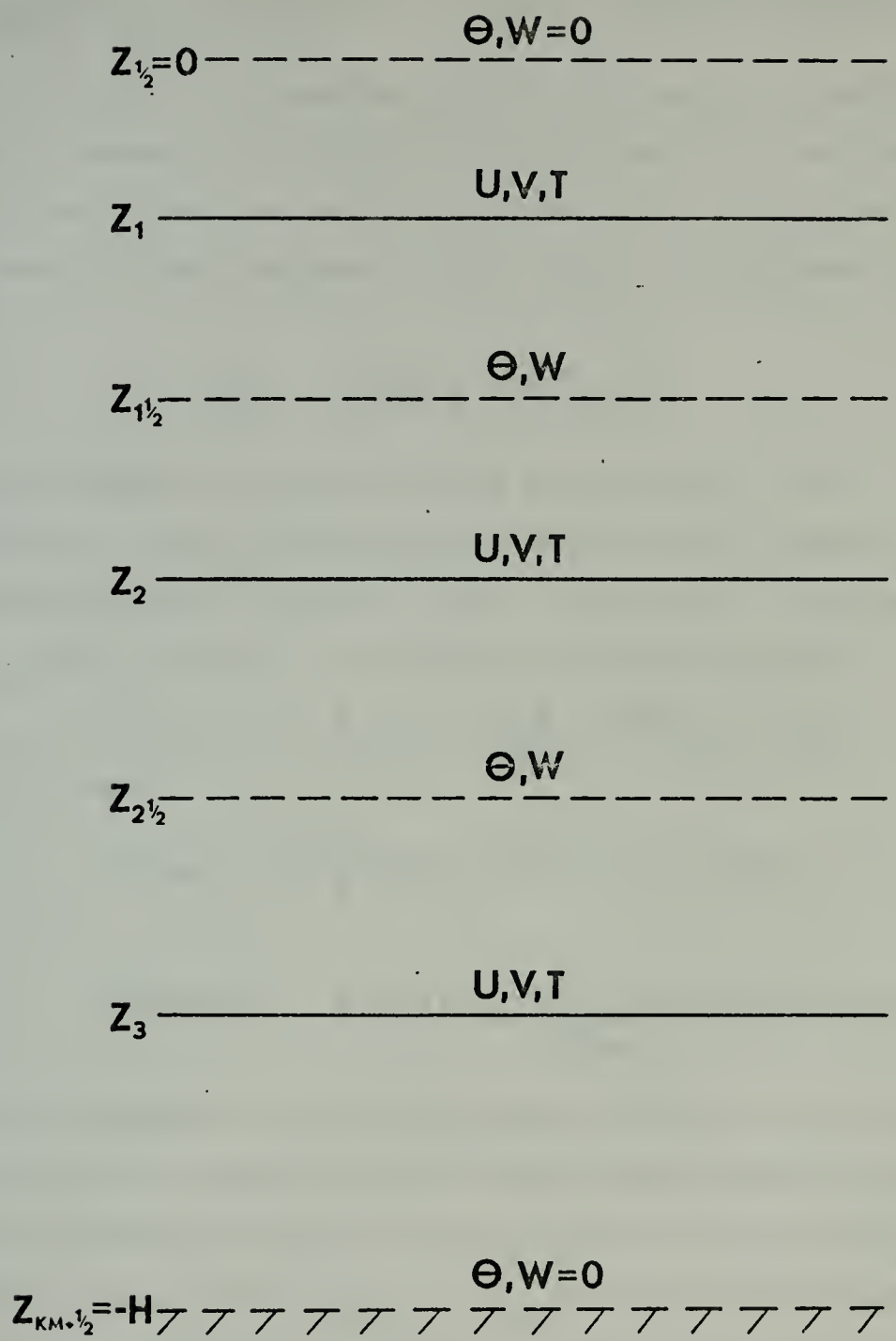

Figure 2. Vertical Placement of Variables

A. NUMERICAL CALCULATION OF AVAILABLE POTENTIAL ENERGY BY HEIGHT PERTURBATION

To calculate the available potential energy by equation (7) it was necessary to calculate the temperature at the boundaries of the layers represented by the subscript k. T_{ijk} represents the vertical mean temperature for a layer of thickness DZ_k where

$$DZ_k = \frac{1}{2}\left[\Delta Z_{k-1/2} + \Delta Z_{k+1/2}\right] .$$

The temperature and height of the water column at the boundaries of each k level were calculated such that T_{ijk} was maintained as a vertical mean. The actual temperatures $\Theta_{ijk-\frac{1}{2}}$, were calculated using the following equations

$$\Theta_{ij1/2} = \frac{2 \cdot T_{ij1} \cdot DZ_1 - \Theta_{ij2} \cdot DZ_{1/2}}{DZ_{1/2}}$$

$$\Theta_{ijk-1/2} = 1/2\left[T_{ijk-1} + T_{ijk}\right] \text{ for } k=2 \text{ to } KM$$

$$\Theta_{ijKM+1/2} = \frac{2 \cdot T_{ijKM} \cdot DZ_{KM} - \Theta_{ijKM} \cdot DZ_{KM-1/2}}{DZ_{KM+1/2}},$$

where KM represents the total number of levels in the model. The horizontal average of the vertical mean temperature, $\overline{T}_k$, was calculated as explained previously. The depth of $\overline{T}_k$ was determined using $\Theta_{ijk-\frac{1}{2}}$ and $Z_{k-\frac{1}{2}}$ by use of the equation

$$Z(\overline{T}_k)_{ijk} = Z_{k-1/2} - \frac{(\Theta_{ijk-1/2} - \overline{T}_k) \cdot (Z_{k-1/2} - Z_{k+1/2})}{\Theta_{ijk-1/2} - \Theta_{ijk+1/2}},$$

where $Z(\overline{T}_k)_{ijk}$ is the depth at which the temperature Θ is equal to the horizontally averaged vertical mean temperature

in the layer k. The horizontal average of the depth of each of the mean temperature surfaces is $\overline{Z(\bar{T}_k)}_k$, and represents the average height of the isotherms between $\bar{\theta}_k$ and $\bar{\theta}_{k+1}$. The departure from the horizontal average was determined as the difference between the temperature surface $Z(\bar{T}_k)_{ijk}$ and its horizontal average $\overline{Z(\bar{T}_k)}_k$. The resulting finite difference analog of (7) for available potential energy was of the form

$$\bar{A} = \frac{g\alpha C_0}{H} \sum_{k=1}^{KM} \frac{1}{2} \overline{Z'^2 (\bar{T}_k)'^2}_{ijk} \cdot \left(\bar{\theta}_{k-\frac{1}{2}} - \bar{\theta}_{k+\frac{1}{2}} \right).$$

B. NUMERICAL CALCULATION OF AVAILABLE POTENTIAL ENERGY BY TEMPERATURE PERTURBATION

Equation (8) shows the analytical forms of the equation for the approximation of average available potential energy using the temperature perturbation, T', instead of the height perturbation, Z'.

The horizontal average temperature, $\bar{T}$, was calculated at each k level. By subtracting this value from the temperature at each grid position, a value for the temperature perturbation, T', was obtained at each grid position. Using these perturbation temperatures, the term $\frac{1}{2}T'^2$ was calculated at each grid position and averaged to the half-integer points $(i+\frac{1}{2}, j+\frac{1}{2}, k+\frac{1}{2})$.

The term for the vertical derivative of the horizontal average temperature was calculated at the i,j integer points

as

$$\frac{\partial \bar{T}}{\partial z}_{k+1/2} \approx \frac{\Delta \bar{T}}{\Delta z}_{k+1/2} = \frac{\bar{T}_k - \bar{T}_{k+1}}{z_k - z_{k+1}} ,$$

and averaged to the half-integer points. The approximation to the mean available potential energy was then obtained by combining these terms and summing over all levels as indicated by

$$APE = \frac{g\alpha\rho_0}{H} \sum_{k=1}^{KM} \frac{\overline{\frac{1}{2}T'^2}_{k+1/2}}{\left(\frac{\partial \bar{T}}{\partial z}\right)_{k+1/2}} \Delta z_{k+1/2} . \qquad (22)$$

C. NUMERICAL CALCULATION OF THE BALANCE OF AVAILABLE POTENTIAL ENERGY

The analytical form of the rate of change of available potential energy is shown by equation (9) as

$$\frac{\partial \bar{A}}{\partial t} = \frac{g\alpha\rho_0}{H} \left[\int_{-H}^{0} \frac{1}{\left(\frac{\partial \bar{T}}{\partial z}\right)} \frac{\partial}{\partial t}\left(\overline{\frac{1}{2}T'^2}\right) dz - \int_{-H}^{0} \frac{\overline{\frac{1}{2}T'^2}}{\left(\frac{\partial \bar{T}}{\partial z}\right)^2} \frac{\partial}{\partial t}\left(\frac{\partial \bar{T}}{\partial z}\right) dz \right] . \qquad (9)$$

The factors $\overline{\frac{1}{2}T'^2}$ and $\partial\bar{T}/\partial z$ in (9), were calculated as in the numerator and denominator of (22). The remaining parts of equation (9) were calculated by use of the right side of the thermodynamic equation as indicated by equations (10) and (11). Equation (10) was written to determine $\frac{\partial}{\partial t}\left(\frac{1}{2}T'^2\right)$ by calculating $T'\frac{\partial T'}{\partial t}$ at integer values of i,j,k and then averaging to obtain its value at half-integer points. Equation (11) was calculated from

$$\frac{\partial}{\partial z}\left(\frac{\partial \bar{T}}{\partial t}\right)_{ijk-1/2} = \frac{\frac{\partial \bar{T}}{\partial t}_{ijk} - \frac{\partial \bar{T}}{\partial t}_{ijk+1}}{z_k - z_{k+1}} ,$$

and then averaged to the half-integer grid points. The resulting finite difference form for equation (9), the balance of domain average available potential energy, is then

$$\frac{\partial \bar{A}}{\partial t} = \frac{g\alpha\rho_0}{H} \sum_{k=1}^{KM-1} \left[\frac{1}{\left(\frac{\partial \bar{T}}{\partial z}\right)_{k+1/2}} \frac{\partial}{\partial t}\left(\frac{1}{2}T'^2\right)_{k+1/2} - \frac{\left(\frac{1}{2}T'^2\right)_{k+1/2}}{\left(\frac{\partial \bar{T}}{\partial z}\right)^2_{k+1/2}} \frac{\partial}{\partial z}\left(\frac{\partial T}{\partial t}\right)_{k+1/2} \right] \Delta z_{k+1/2} . \quad (23)$$

D. NUMERICAL CALCULATIONS OF THE TERMS FOR THE BALANCE OF AVAILABLE POTENTIAL ENERGY

As indicated by equation (21), the balance of mean available potential energy contains five terms which are obtained by use of the thermodynamic equation (5). Development of equation (21) showed that the five terms could be written as below

$$-\overline{T'w\frac{\partial \bar{T}}{\partial z}} = \overline{T'\left[-\nabla\cdot(w\bar{T}) - \frac{\partial(w\bar{T})}{\partial z}\right]} \quad (18)$$

$$-\overline{\frac{\partial}{\partial z}\left(\frac{wT'^2}{2}\right)} = \overline{T'\left[-\nabla\cdot(wT') - \frac{\partial(wT')}{\partial z}\right]} \quad (19)$$

$$\overline{\frac{T'Q'}{\rho_0 c}} = \overline{T'\left[\left(A_H\nabla^2 T\right)' + \left(K_t\frac{\partial^2 T}{\partial z^2}\right)' + \delta_c(T)'\right]} \quad (20)$$

$$\frac{\partial}{\partial z}\left(-\frac{\partial \overline{(wT)}}{\partial z}\right) = \overline{\frac{\partial}{\partial z}\left(-\frac{\partial(wT)}{\partial z}\right)} \quad (24)$$

$$\frac{\partial}{\partial z}\left(\frac{\bar{Q}}{\rho_0 c}\right) = \overline{\frac{\partial}{\partial z}\left[K_t\frac{\partial^2 T}{\partial z^2} + \delta_c(T)\right]} . \quad (25)$$

The terms in the brackets on the right side of the above five equations were calculated using the identical finite difference method as used in the general circulation model to calculate the terms of the thermodynamic equation. The details are in Haney (1974).

V. RESULTS

To make an accurate comparison of the two expressions for domain average available potential energy, equations (7) and (8), and to determine the importance of the terms occurring in the balance of available potential energy, equation (21), the general circulation model, as described in chapter II, was run for large-scale motion. A description of the conditions and the results obtained are given below.

A. GENERAL CIRCULATION MODEL OF THE OCEAN

To establish quasi-steady state conditions, the model, Haney (1974), was run in two phases. For the first phase, the linearized form of the vertical shear current was used. The vertical shear current equations were obtained from the primitive equation form of the horizontal equations of motion, (1) and (2), by subtracting the vertical mean of equation (1) from equation (1) and by subtracting the vertical mean of equation (2) from equation (2). The vertical mean current is assumed constant in time. The temperature is determined from the complete thermal equation (5). The first phase integration was for approximately 100 years. For the second phase, the complete nonlinear equations were used. The second phase integration was for 25 years. A more complete description of phase 1 and phase 2 may be found in Haney (1974). Twenty-four sets of model history data was taken at this point at intervals

of 25 days, representing a total of 600 days. The results showed the motion to be not strictly steady-state. As shown by Haney (1974), slight warming was occurring near the bottom after the integration period indicating a continuing downward flux of heat. Figure 3 shows the temperature at 20 meters below the surface, averaged over the last year of integration for phase 2. Figure 4 shows the vertical velocity at 60 meters below the surface averaged over the last year of the second phase. Comparing figures 3 and 4 shows two large gyres centered on each side of the equator. In these gyres, warm water is being forced down. Near the equator and along the northern and southern boundaries, cold water is being forced upward. Thus, available potential energy is being generated by these motions.

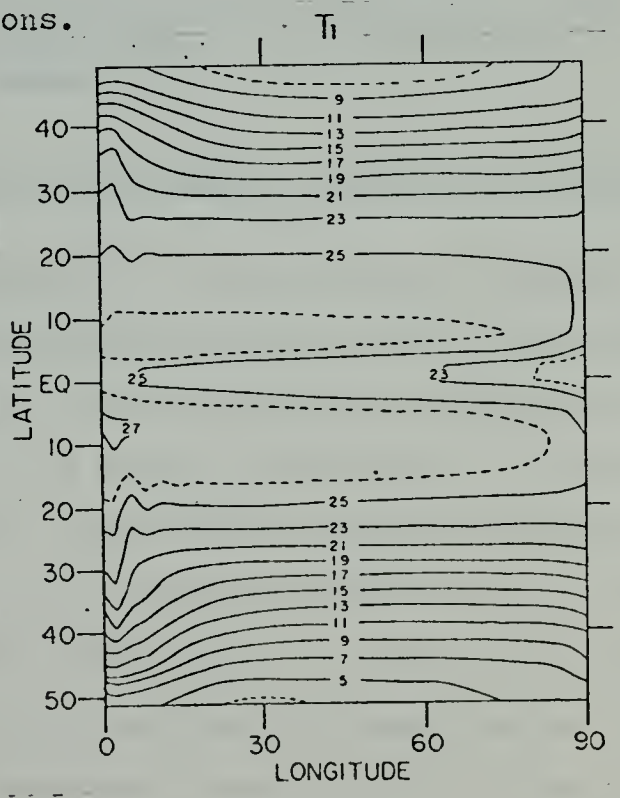

Figure 3. Temperature (^{o}C) at 20 m, averaged over the last year of the second phase.

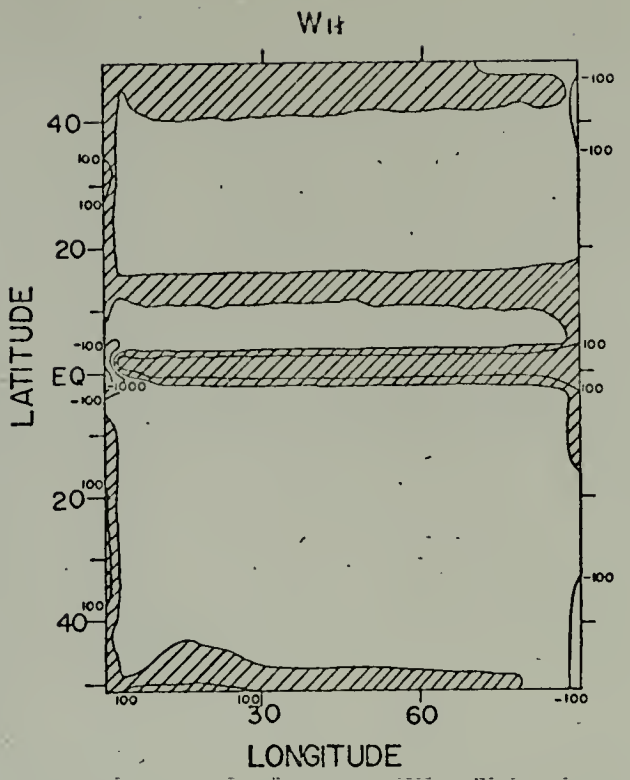

Figure 4. Vertical velocity (cm day^{-1}) at 60 m, averaged over the last year of the second phase. Upward motion is shaded.

1. Results of Available Potential Energy Calculations

Comparison of calculations of available potential energy as determined by equation (8) and the approximate form (9) showed that the available potential energy as calculated by the height perturbation to be slightly larger, (1383 ergs/cm^3), than the available potential energy as calculated by the temperature perturbation, (1232 ergs/cm^3), figure 5. This discrepancy is perhaps due to Tmax and Tmin being not uniquely defined in Z coordinates. Fluctuations in available potential energy due to a minor change in the model near the end of the 600 day period of record were

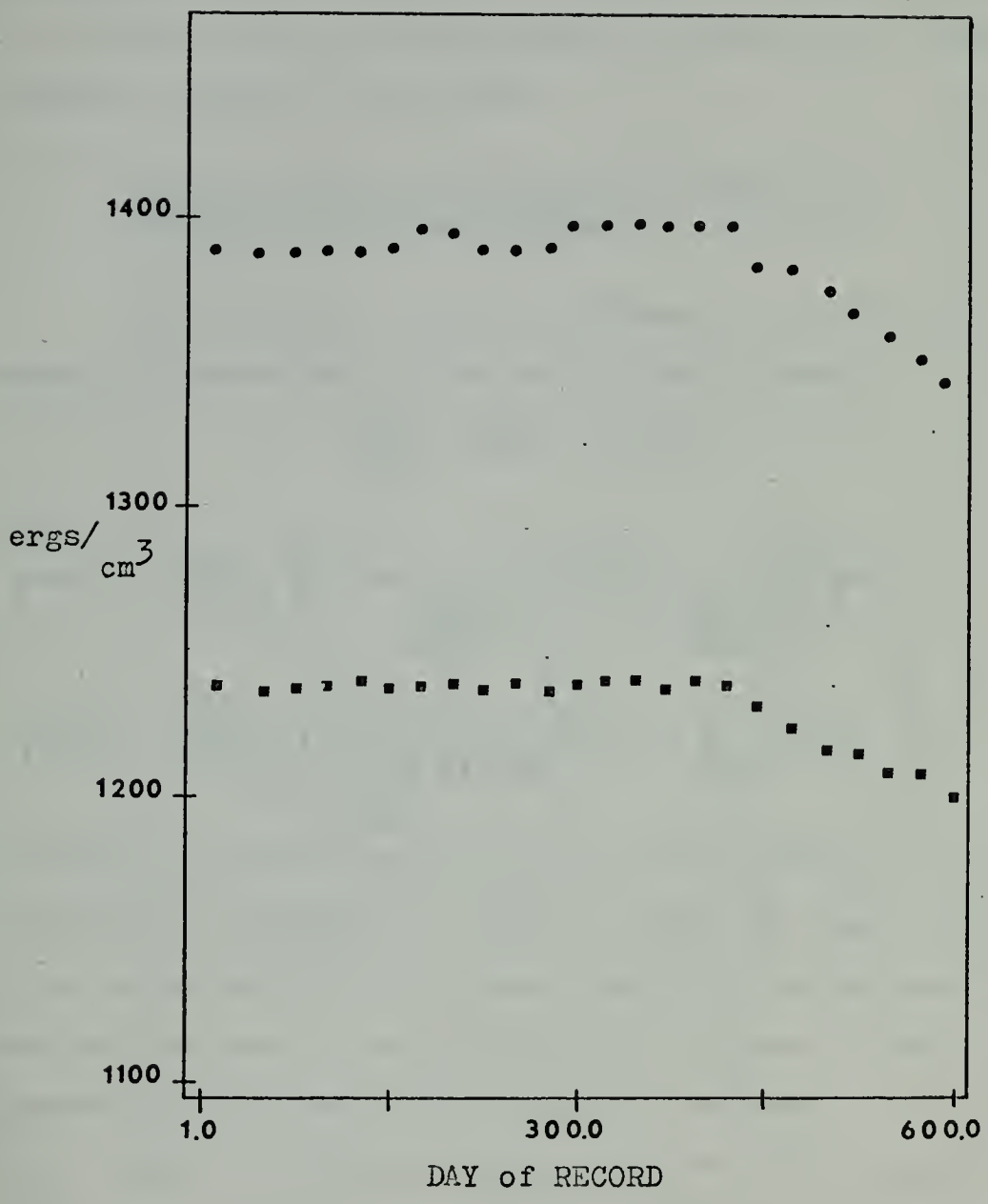

Figure 5. APE by $\overline{\frac{1}{2}Z'^2}$(•) and by $\overline{\frac{1}{2}T'^2}$(▪) for the General Circulation Model.

simulated by both forms of available potential energy calculations. Figure 5 indicates equation (8) calculated available potential energy to a sufficient degree of accuracy to be considered a good approximation equation for available potential energy in this model.

2. Results of Calculations of the Balance of Available Potential Energy

From equation (21), the balance of available potential energy is represented by the sum of two integrals,

$$\frac{\partial A}{\partial t} = \text{part 1} - \text{part 2}$$

where

$$\left.\begin{aligned} \text{part 1} &= \frac{g\alpha\rho_0}{H}\int_{-H}^{0}\Bigg[\underbrace{-\overline{T'w}}_{1.} - \underbrace{\frac{1}{\left(\frac{\partial\bar{T}}{\partial z}\right)}\frac{\partial}{\partial z}\left(\frac{\overline{wT'^2}}{2}\right)}_{2.} + \underbrace{\frac{1}{\left(\frac{\partial\bar{T}}{\partial z}\right)}\frac{\overline{T'Q'}}{\rho_0 C}}_{3.}\Bigg]dz \\ \text{part 2} &= \frac{g\alpha\rho_0}{H}\int_{-H}^{0}\Bigg[\underbrace{\frac{\tfrac{1}{2}\overline{T'^2}}{\left(\frac{\partial\bar{T}}{\partial z}\right)^2}}_{4.}\frac{\partial}{\partial z}\Bigg[\underbrace{-\frac{\partial}{\partial z}(\overline{wT})}_{4.} + \underbrace{\frac{\bar{Q}}{\rho_0 C}}_{5.}\Bigg]\Bigg]dz . \end{aligned}\right\} \quad (26)$$

According to their definitions, Q' and $\bar{Q}$ contain the convective adjustment of temperature, $\delta_c(T)'$, and $\delta_c(\bar{T})$ respectively. In the calculations below, these convective adjustment terms were omitted due to the difficulty of recovering this irreversible process from the history records.

Part 1 represents changes in available potential energy resulting from changes in the variance of the temperature perturbation on a horizontal surface. Heating of warmer regions and cooling of colder regions at the same depth increases the horizontal temperature variance and increases available potential energy. Part 2 represents changes in

available potential energy due to changes in mean static stability. Heating of upper levels and cooling of lower levels increases the static stability and decreases available potential energy. The magnitude of these integrals are shown by figure 6. Variations in these two parts after day 400 of the history record were caused by the fact that the convective adjustment, $\delta_c(T)$, was changed to double precision accuracy in the model.

The processes represented by part 1 are serving to decrease the total available potential energy in this model, indicating the model, apart from $\delta_c(T)'$, is working to reduce temperature perturbations. The magnitude of the three terms comprising part 1, equation (26), are shown in figure 7, where all three terms are of the same order of magnitude. The first term of part 1 shows the transformation of energy between available potential energy and kinetic energy due to a correlation between the temperature perturbation and vertical velocity. Results indicate that in the domain average, energy is being transformed from kinetic energy to available potential energy. This is consistent with the results of Haney (1974), as discussed above, where a transformation of kinetic energy of vertical shear motion to potential energy was occurring. Term 2 represents a triple correlation due to convergence of the vertical flux of temperature fluctuations. Being a triple correlation of perturbation quantities, Lorenz (1955) assumed this term to be negligible in the atmosphere. In

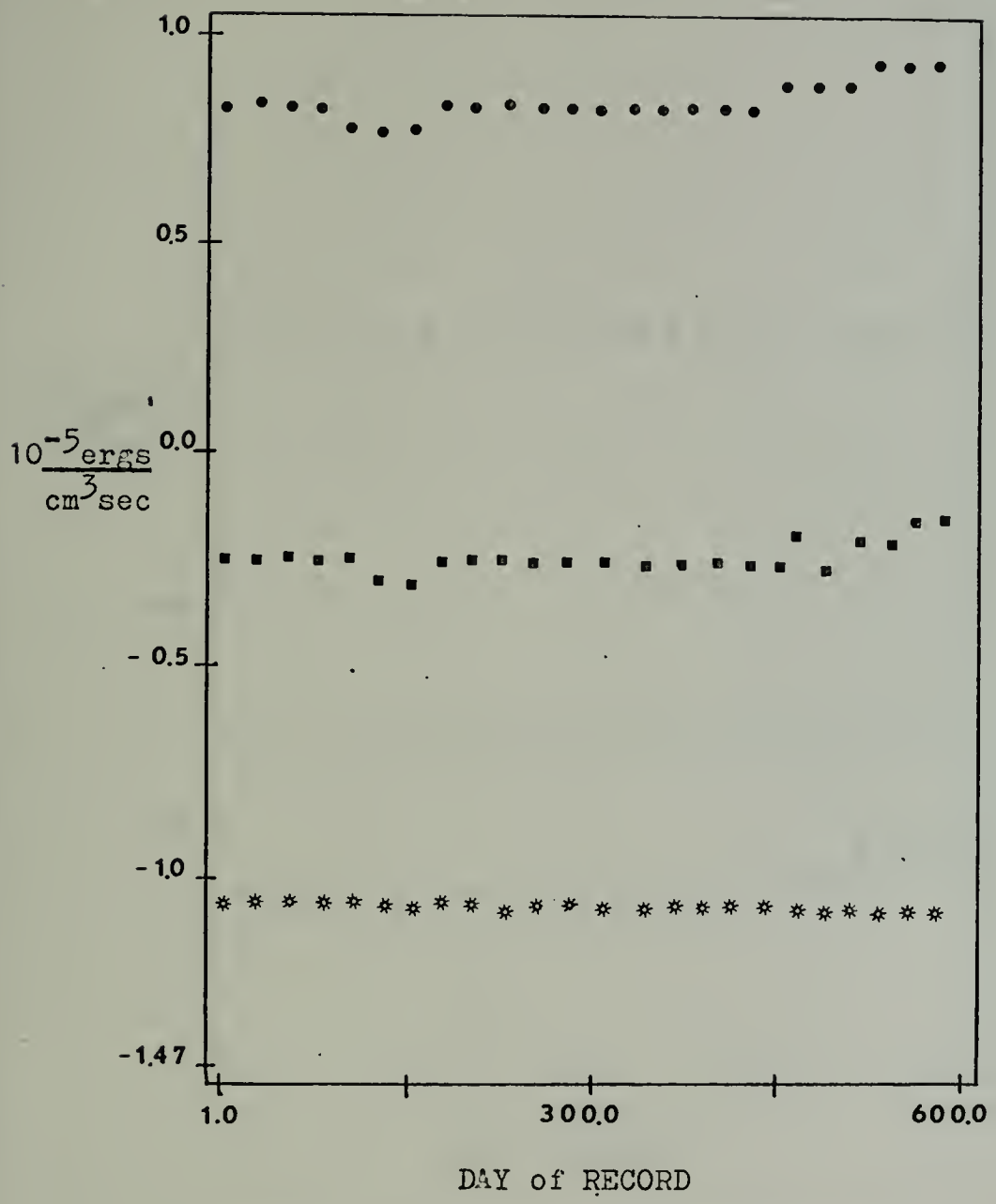

Figure 6. The Values of (Part1-Part2, •) and the Values of Part1(▪) and Part2(*) of Eq. (26) vs. Time.

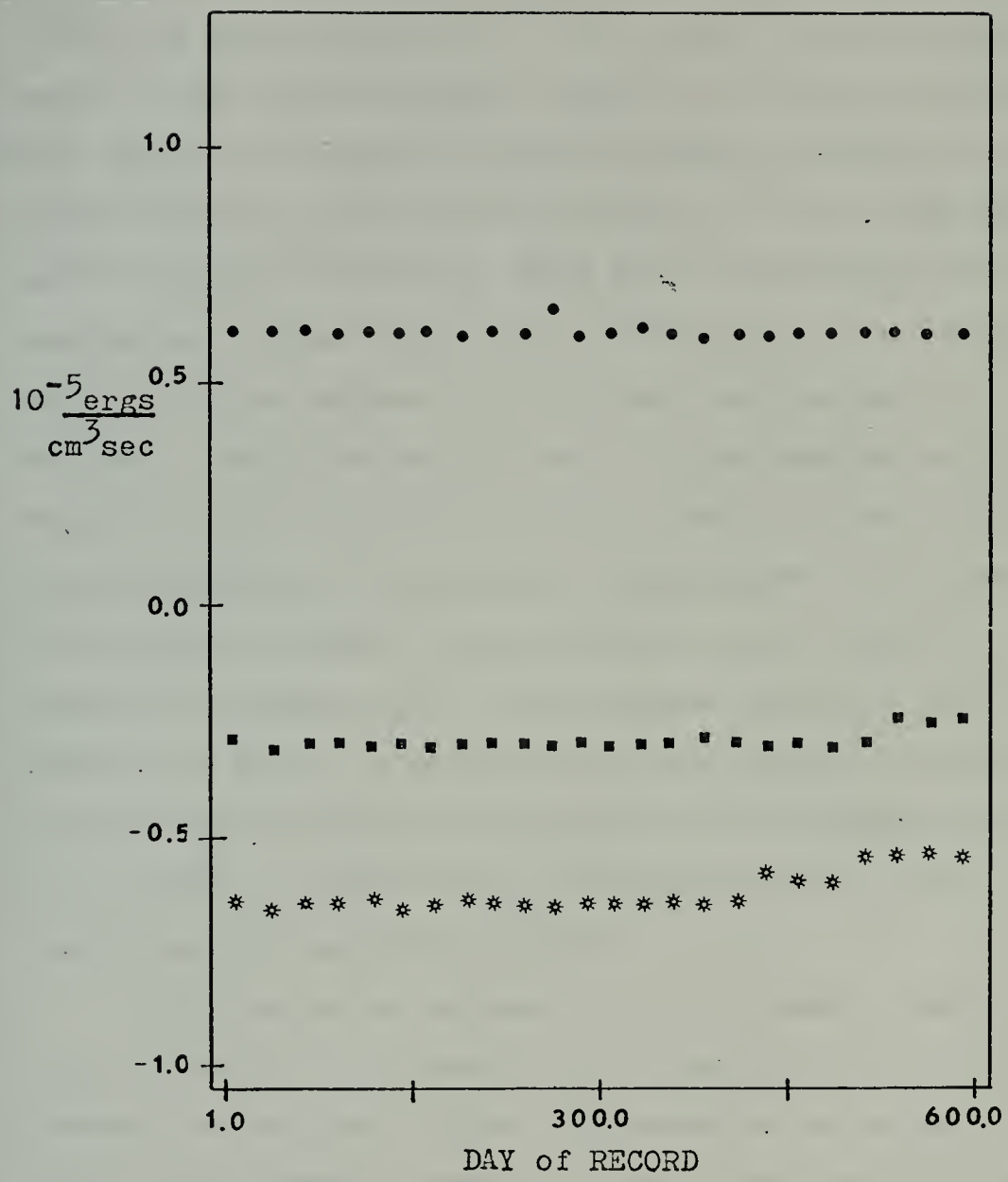

Figure 7. Contribution by Term1(•), Term2(▪), Term3(*) to the Balance of APE, Eq. (26).

this general circulation model, term 2 is smaller than all of the other terms by only a factor of 2 to 3 and thus it cannot be neglected. This term arises because the static stability, $\partial\overline{T}/\partial Z$, is not constant in Z. If it were, the term would vanish. The term would also vanish if the triple correlation were small. One reason it was not small is because of the forced nature of the vertical velocity, w, and temperature fields near the boundaries. With heat flux through the boundaries, neither the vertical velocity nor the temperature gradient in the horizontal would have been as large as occurred. The third term of part 1 shows generation of available potential energy due to a spatial correlation between heating and perturbation temperature. This term was calculated without the contribution from $\delta_c(T)'$, present in equation (20). The negative result of term 3 indicates a loss of available potential energy due to the non-convective heating. The magnitude of this term indicates the importance of the thermal diffusion terms in this oceanic general circulation model.

The processes represented by the terms of part 2, figure 8, were of the same order of magnitude, and tend to increase the available potential energy in the model. The first term of part 2, term 4, is due to the vertical flux of mean temperature and the second term, term 5, is due to mean heating. As in term 3, the convective adjustment term, $\delta_c(\overline{T})$, was absent from the mean heating term. $\delta_c(\overline{T})$ tends to increase the mean static stability, $\partial\overline{T}/\partial Z$, and to

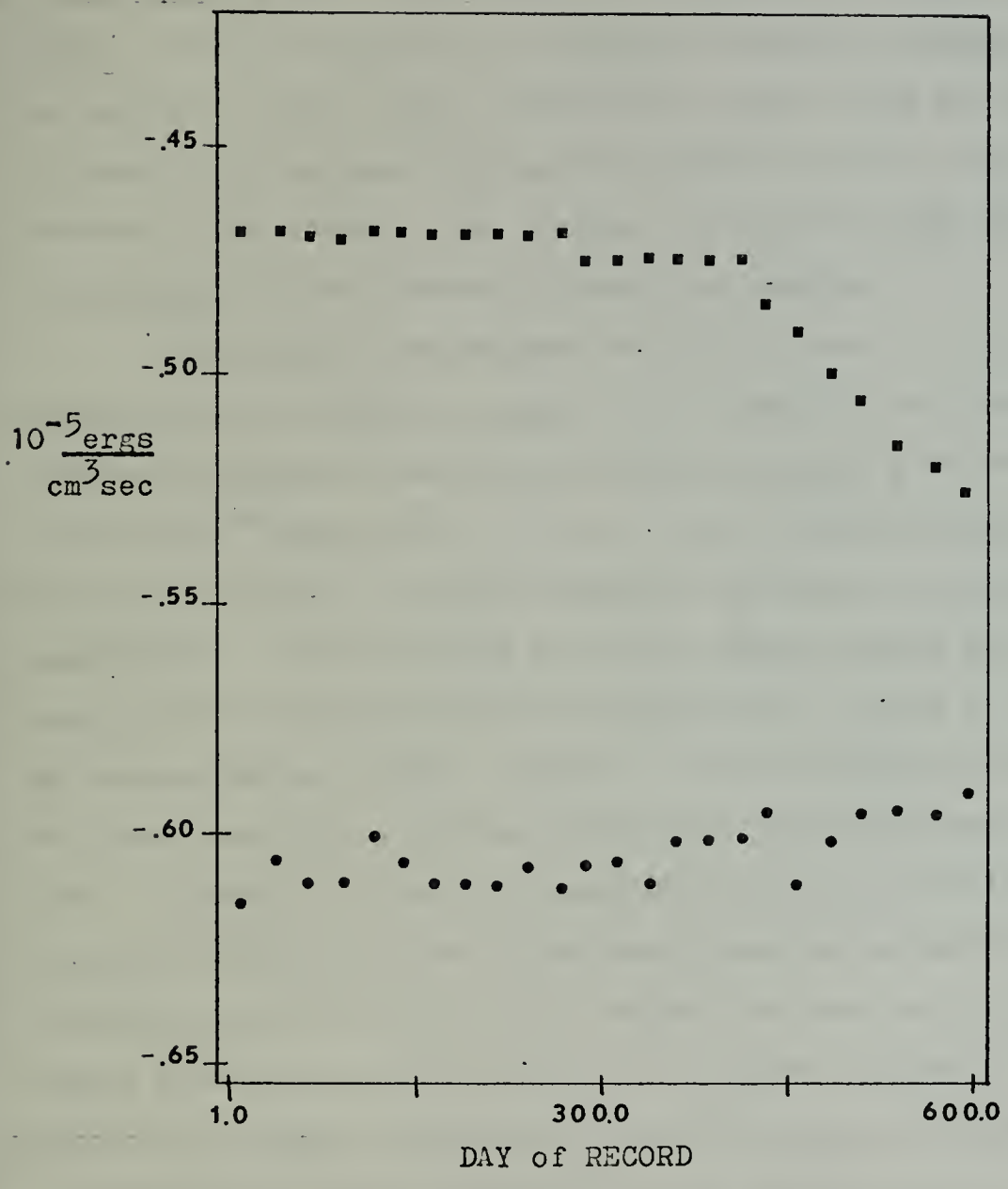

Figure 8. Contribution by Term4(•) and Term5(*) to the Balance of APE, Eq. (26).

decrease available potential energy. It's inclusion would allow terms 4 and 5 to sum to a negligible value. Lorenz (1955) assumed part 2 was zero for steady-state atmospheric motion. Under conditions of seasonal radiation heating, the vertical flux of mean temperature, term 4, may not be in phase with the mean heating that occurs, term 5, and thus would not cancel. The general circulation model was not designed to show seasonal radiation heating.

The energy flow diagram depicting terms 1 - 5 in equation (26) is shown in figure 9. Terms 1,4 and 5 were serving to increase available potential energy by an amount of 1.705×10^{-5} ergs/cm^{3}sec. Terms 2 and 3 were serving to decrease available potential energy by an amount of $.908 \times 10^{-5}$ ergs/cm^{3}sec. The available potential energy during the record period was observed to be decreasing, figure 5, with an average value of 1232. ergs/cm^3. The discrepancy between the terms serving to increase available potential energy, part 1 - part 2 $>$ 0, and the observed decrease in available potential energy, figure 5, was determined to be due to not including the $\delta_c(T)$ term in the balance of available potential energy calculations. The value of the term required to balance the energy flow diagram, as in steady-state conditions, is indicated by term 6 and shown by the dashed line in figure 9 to be approximately $.797 \times 10^{-5}$ ergs/cm^{3}sec. These results indicated convective adjustment was an important process in the model, as was expected since the model contained a large region of near isothermal water at high

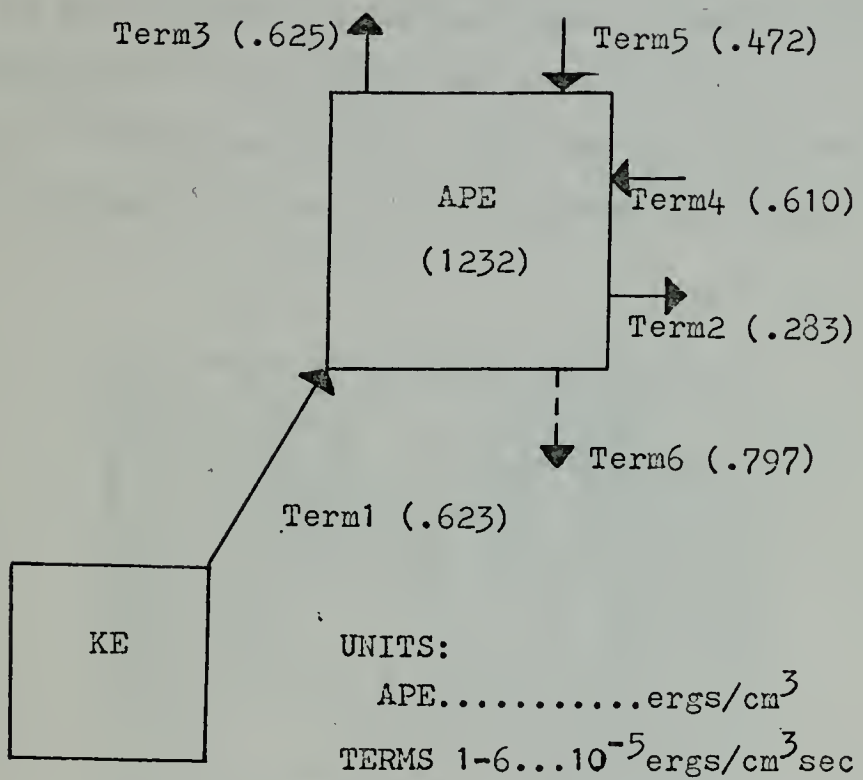

Figure 9. Energy Flow Diagram for the General Circulation Model.

latitudes where convective adjustment would frequently occur. The convective overturning plays no role in the kinetic energy budget and therefore the arrow for term 6 shows this effect to be an external loss to the system.

B. MID-OCEAN DYNAMICS EXPERIMENT MODEL

Figure 10 below shows the instantaneous streamfunction for day 10080 during the seventh year of fine grid calculations. Twenty-four sets of data for the experiment were taken from day 10050 to 10110 at $2\frac{1}{2}$ day intervals.

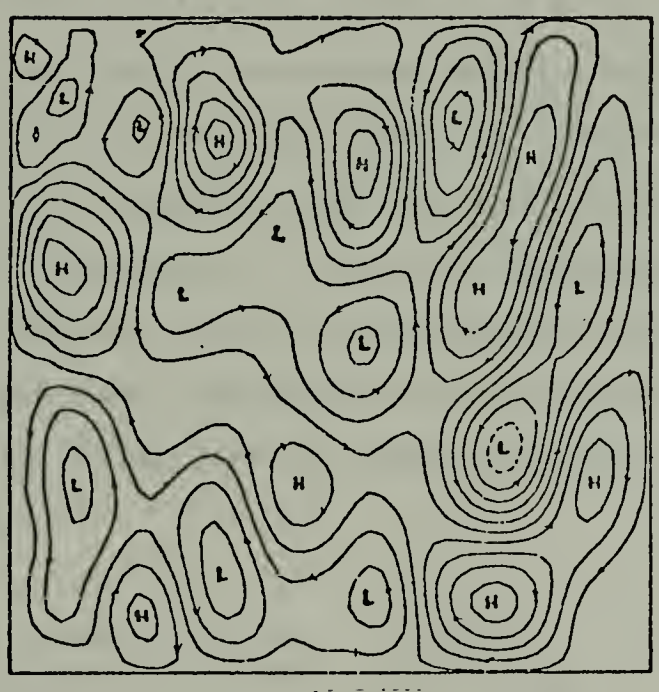

Figure 10. Instantaneous streamfunction for day 10080 of the Mid-Ocean Dynamics Experiment Model.

To determine the available potential energy as a result of transient motion and standing motion, equation (8) was written with temperature in terms of a time average temperature, $[T]$, for standing motion, and a departure from the time average, T^*, for transient motion. Since available potential energy is determined from the temperature perturbation, the horizontal average of the time averaged temperature was determined. Then the perturbation temperature of the standing motion, $[T]'$ and transient motion, $T^{*'}$, was determined as below

$$T = [T] + T^*$$
$$T = \overline{[T]} + \overline{T^*} + [T]' + T^{*'}, \qquad (27)$$

where $[\bar{T}]$ is the horizontal averaged standing temperature and $\overline{T^*}$ is the horizontal averaged transient temperature. The term $[T]'$ is the standing eddy temperature and $T^{*'}$ is the transient eddy temperature. The eddy temperature is then the sum of the last two terms of equation (27). Substitution of the eddy temperatures into equation (8) resulted in the following form for domain average available potential energy,

$$APE \approx \frac{g\alpha\rho_0}{H}\int_{-H}^{0}\left\{\frac{1}{2}\overline{[T]'^2} + \frac{1}{2}\overline{[T]'T^*} + \frac{1}{2}\overline{T^{*'2}}\right\}\frac{dz}{\left(\frac{\partial\bar{T}}{\partial z}\right)}. \qquad (28)$$

The time averaged available potential energy was written as

$$[APE] \approx \frac{g\alpha\rho_0}{H}\int_{-H}^{0}\left\{\frac{1}{2}\overline{[T]'^2} + \frac{1}{2}\overline{[T^{*\prime 2}]}\right\}\frac{dZ}{\left[\frac{\partial\bar{T}}{\partial Z}\right]}, \qquad (29)$$

where the term $\overline{\left[\frac{1}{2}[T]'T^{*\prime}\right]}$ vanishes. In this model, the static stability factor $[\partial T/\partial Z]$ was assumed constant in time and written as γ. Equation (29) shows time average available potential energy as the sum of a part due to the standing field and a part due to the transient motion.

For the study of the balance of available potential energy in the mid-ocean dynamics experiment model, only the first three terms of equation (21) were considered important for further study. Because lateral boundary conditions allowed heat to flow in or out of the model, it was reasoned that convective adjustment would not play an important role in the model. With little convective adjustment and steady forcing, it was therefore assumed that the long-time average of the sum of terms 4 and 5, part 2 of equation (26), would be negligible. Calculations of the balance of total available potential energy, below, showed the terms of part 2 summed to approximately zero for each set of data as well as in a time average so the assumption was justified. The study therefore concentrated on transformations of energy due to $\overline{\frac{1}{2}T'^2}$. From the first three terms of equation (21), the balance of available potential energy was approximated as

$$\frac{\partial A}{\partial t} \approx \frac{g\alpha\rho_0}{H}\int_{-H}^{0}\left\{-\overline{T'w'} - \frac{1}{\left(\frac{\partial\bar{T}}{\partial z}\right)}\frac{\partial}{\partial z}\left(\frac{\overline{wT'^2}}{2}\right) + \frac{1}{\left(\frac{\partial\bar{T}}{\partial z}\right)}\frac{\overline{T'Q'}}{\rho_0 C}\right\}dz \qquad (30)$$

1. 2. 3.

Equation (30) was written in terms of a part due to transient motion, q^*, and a part due to standing motion, $[q]$, for a quantity q and then time averaged as

$$\left[\frac{\partial A}{\partial t}\right] \approx \frac{g\alpha\rho_0}{H}\int_{-H}^{0}\left\{-\overline{[w]'[T]'} - \overline{[w^{*'}T^{*'}]} - \frac{1}{\gamma}\frac{\partial}{\partial z}\left(\frac{1}{2}\overline{[w]'[T]'[T]'} + \frac{1}{2}\overline{[w^{*'}T^{*'}T^{*'}]}\right.\right.$$

1a. 1b. 2a. 2b.

$$\left.\left. + \frac{1}{2}\overline{[w][T^{*'}T^{*'}]} + \overline{[w^{*'}T^{*'}][T]'}\right) + \frac{1}{\gamma}\overline{[T][Q]'} + \frac{1}{\gamma}\overline{[T^{*'}Q^{*'}]}\right\}, \qquad (31)$$

2c. 2d. 3a. 3b.

where the quantities containing only one term due to transient motion were zero in the long-time average. The values of terms 2c and 2d were not calculated in this study but their sum could be inferred from terms 2, 2a and 2b. Since heat diffusivity was allowed across the boundaries, the definition of $\overline{Q}/\rho_0 c$ in (25) was changed to the following

$$\frac{\overline{Q}}{\rho_0 C} = \left(\overline{A_H \nabla^2 T}\right) + \left(\overline{K\frac{\partial^2 T}{\partial z^2}}\right) + \overline{\delta_c(T)}$$

since $\overline{A_H \nabla^2 T}$ was not equal to zero in the MODE model.

1. Results of Available Potential Energy Calculations

Figure 11 shows the total available potential energy as determined from equation (28) to be slowly increasing during the history record. The first term on the right side

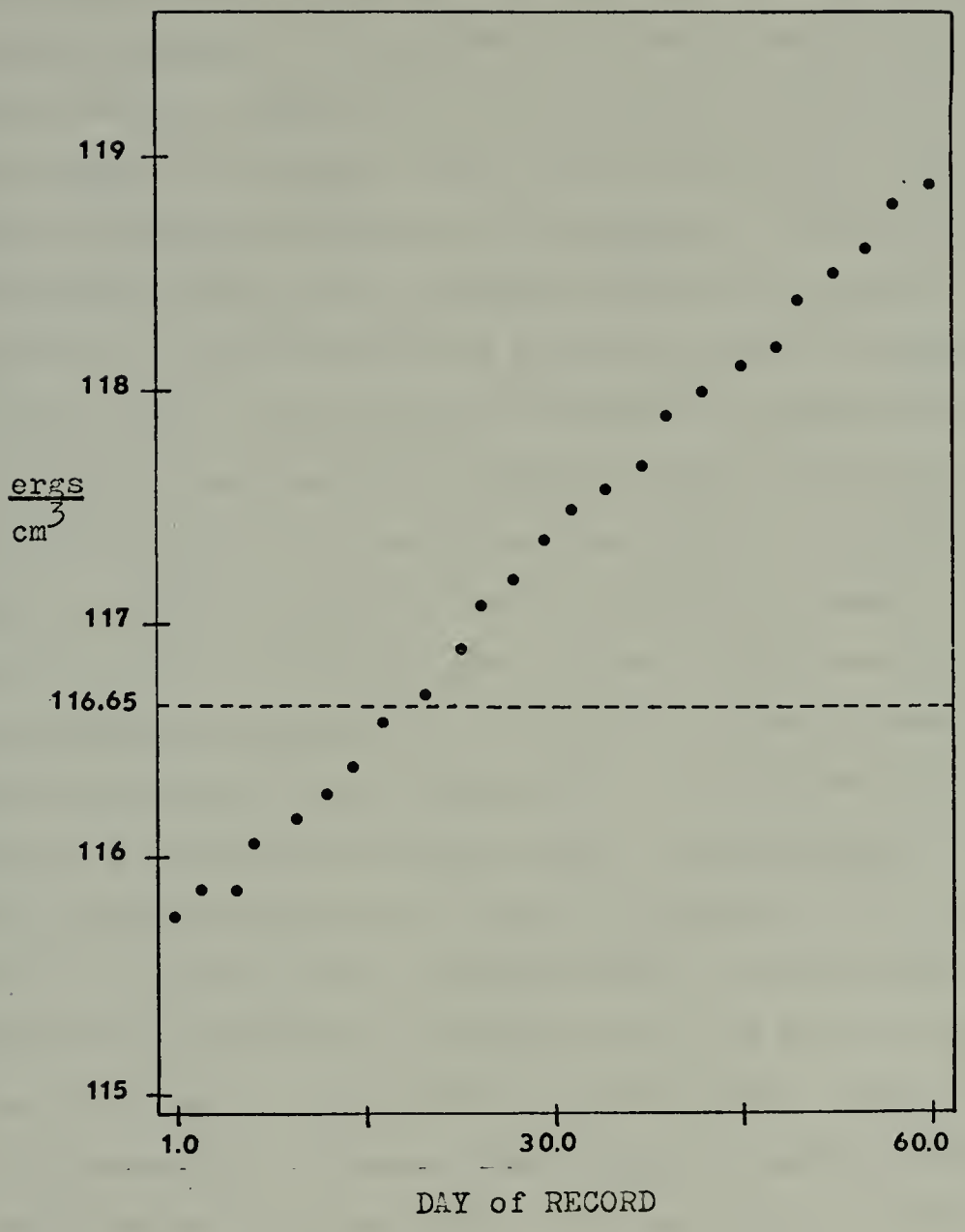

Figure 11. APE vs. Time for the MODE Model (Total Motion)

of equation (28), due to standing motion was constant in time and had a value equal to 116.65 ergs/cm^3, shown in figure 11. This was an order of magnitude smaller than the available potential energy of the general circulation model and it points out the importance of the horizontal diffusion of heat across the northern and southern boundaries in preventing large horizontal gradients of temperature. The third term of equation (28), due to transient motion, is shown in figure 12. This term appears to have a period of approximately 100 days, but is too small in amplitude to significantly affect the total available potential energy. Since the left side of equation (28) was known from figure 11, and two terms on the right side of equation (28) were known, the middle term on the right side of equation (28) was found to be primarily responsible for the slow increase of available potential energy seen in figure 11. The time average of the total available potential energy, corresponding to the left side of equation (29) was 117.3 ergs/cm^3. The first term on the right side of equation (29), the available potential energy due to standing motion, is the same as the first term on the right side of equation (28), equal to 116.65 ergs/cm^3. Thus the time average available potential energy due to transient motion, the last term of equation (29), had a value of .66 ergs/cm^3 and was only a small part of the time average total available potential energy. Being so small, the available potential energy due to transient motion would probably not be noticed on a temperature map

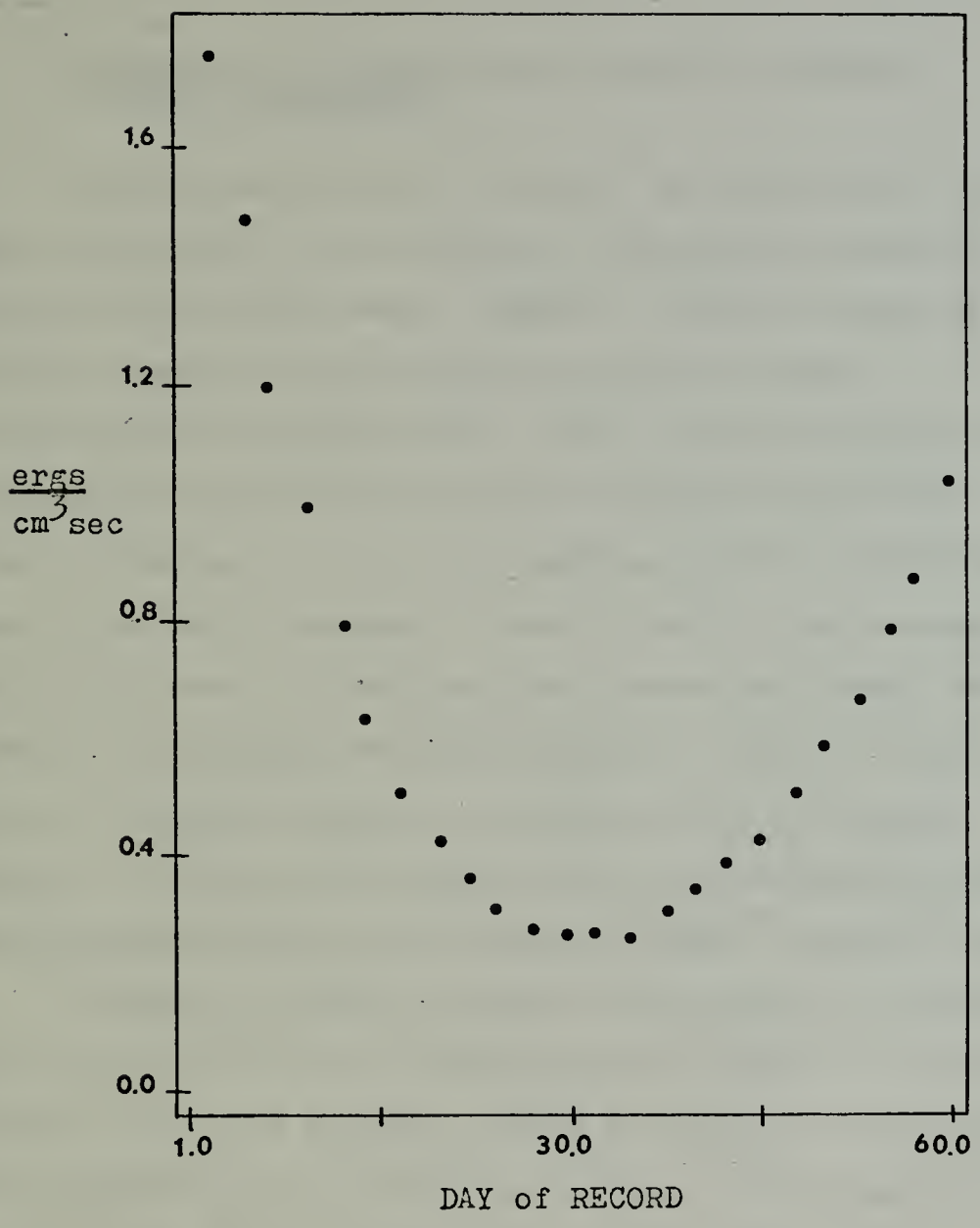

Figure 12. APE by $\overline{\frac{1}{2}T'^2}$ vs. Time for the MODE Model (Transient Motion)

from the model. If the variations in kinetic energy were of this order of magnitude, it could be important in the kinetic energy balance which would be subject to future investigation.

2. Results of the Balance of Available Potential Energy Calculations

By the use of flow diagrams, the magnitude of the terms responsible for the balance of available potential energy can be easily seen. Figure 13 shows the balance of the time average total available potential energy, corresponding to equation (30). This figure indicates energy was being transformed from kinetic energy to available potential energy by term 1 of equation (30) at a rate faster than it was being removed by terms 2 and 3. The average rate of increase of total available potential energy, as shown in the diagram, was approximately $.046 \times 10^{-5}$ ergs/cm^{3}sec. From the observed change in available potential energy, figure 11, there was an average rate of available potential energy change during the 60 days of $.05 \times 10^{-5}$ ergs/cm^3 sec.

Figure 14 shows the value of the energy transformations due to standing motion, corresponding to terms 1a, 2a, 3a of equation (31), and figure 15 shows the value of the energy transformations due to transient motion, corresponding to terms 1b, 2b, 3b of equation (31). The average rate of increase of available potential energy by the standing field, as shown in the diagram, was approximately $.075 \times 10^{-5}$ ergs/cm^3 sec. The average rate of decrease by the transient field, as shown in the diagram, was $.035 \times 10^{-5}$ ergs/cm^3 sec.

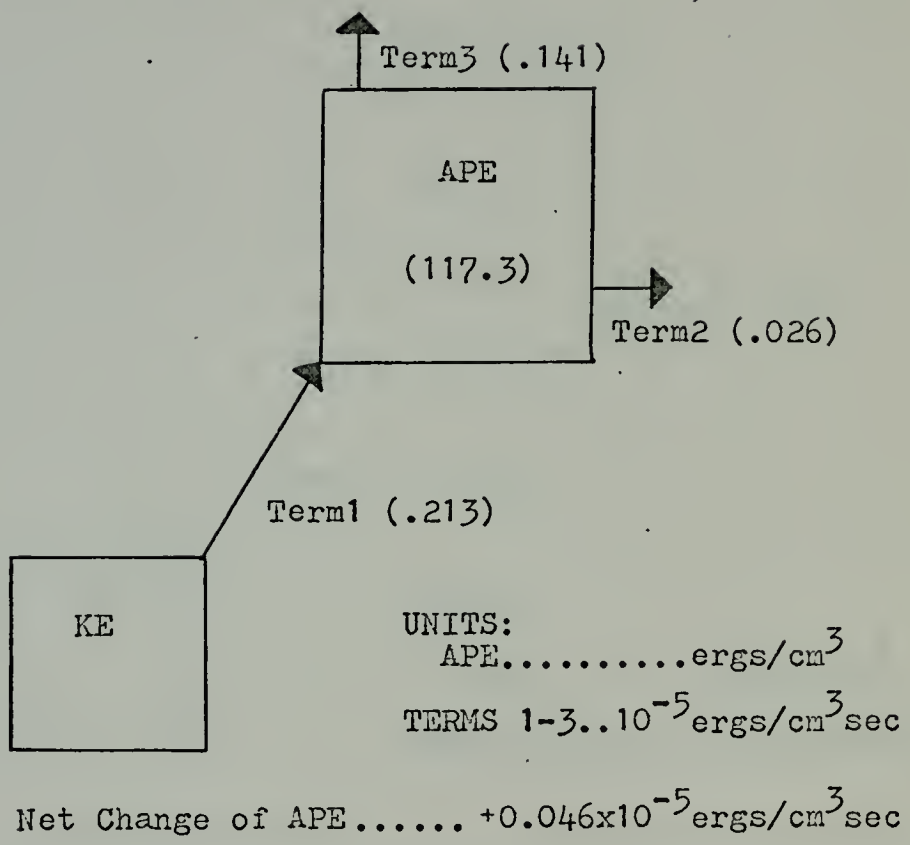

Figure 13. Energy Flow Diagram for the MODE Model (Total Motion Eq. 30)

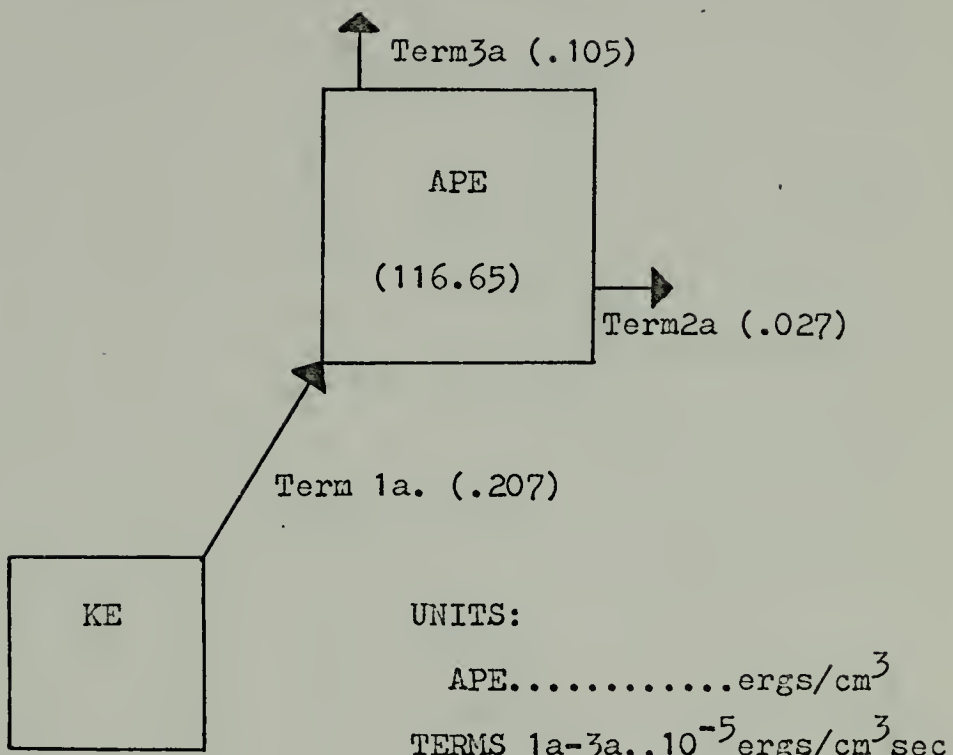

Figure 14. Energy Flow Diagram for the MODE Model (Standing Motion, Eq. 31)

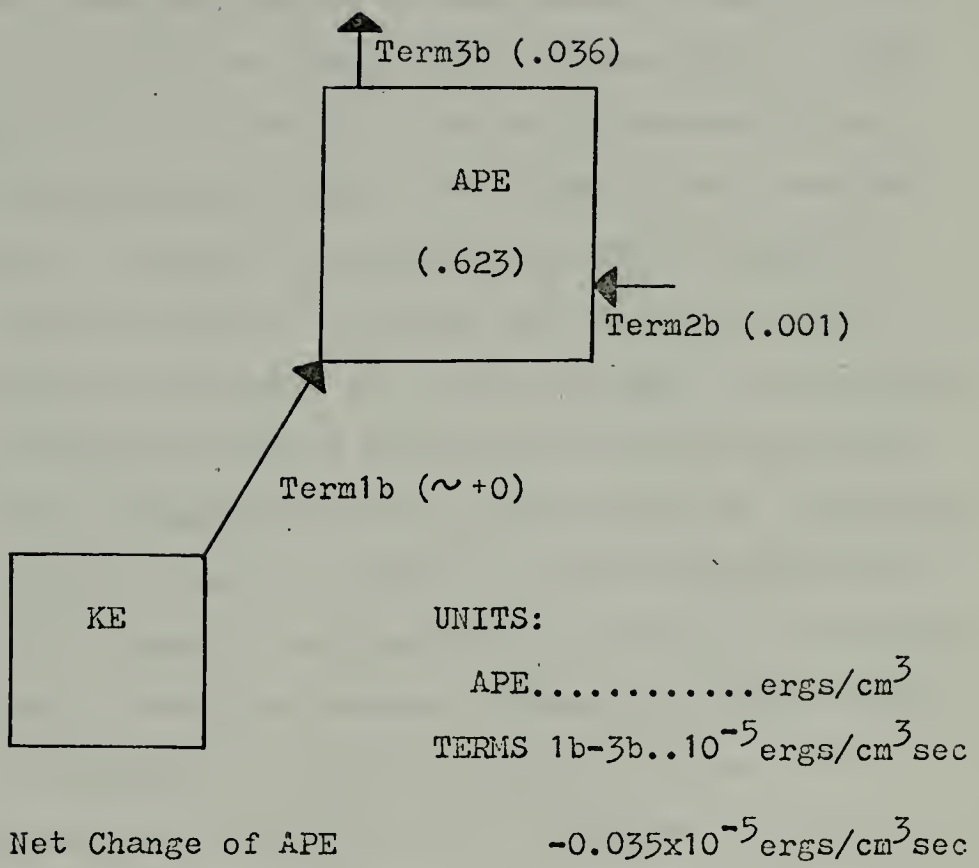

Figure 15. Energy Flow Diagram for the MODE Model (Transient Motion, Eq. 31)

Instead of such changes in the available potential energy fields, this perhaps simply indicates that a conversion of available potential energy from the standing to the transient fields was occurring. The conversion term for available potential energy between the standing and transient fields was not calculated because it also contained terms of standing and transient motion as does terms 2c and 2d. The conversion term must have had a value between .035 to .075 $x10^{-5}$ ergs/cm^3 sec. Summing of the net increases by the standing field and the transient field gave a net increase for the total of .040$x10^{-5}$ ergs/cm^3 sec, which compares with the value of .046$x10^{-5}$ ergs/cm^3 sec seen in figure 13. The sum of terms 3a, figure 14, and 3b, figure 15, was equal to term 3 of figure 13 as it should be, since in the time average term 3 is composed of only term 3a and 3b. Similarly, term 2a, figure 14, and 2b, figure 15, sum to equal term 2 of figure 13. However, from equation (31) term 2 is composed of four terms in the time average. Therefore, terms 2c and 2d must be negligible or sum to a negligible value.

The sum of 1a and 1b is less than term 1 by an amount of .006$x10^{-5}$ ergs/cm^3 sec. Some round-off errors may have occurred to cause the small discrepancy. Comparing figure 13 and figure 14, the total energy being transformed from kinetic energy to available potential energy, term 1, was almost totally by the standing field, term 1a. Since term 1b, figure 15, was small and positive, the source of kinetic energy for the transient motion was not available

potential energy during the 60 day period of the MODE model. Figure 16 shows the total transformation from kinetic energy to available potential energy, term 1, was undergoing large fluctuations. At some times the transient eddies did draw energy from available potential energy, since 1b, figure 17, was at times negative, but the energy flow in either direction was small. These results may indicate that the transient eddies were not baroclinic for the 60 day period. The amplitude of the eddies of the MODE model were known to be large. With large amplitude eddies, the dissipative forces were expected to be large, indicating the transformation of energy from the source of energy for the kinetic energy of the eddies was large. Therefore the primary source of energy for the transient eddies was not available potential energy during the 60 day history record.

It was suspected that errors may have occurred due to the $2\frac{1}{2}$ day rate of sampling the data. Figure 16 shows the three terms of equation (30) as a function of time. Term 1 and 2 fluctuate to a greater extent than term 3. Since both term 1 and 2 are correlated with vertical velocity, w, the possibility of aliasing is further supported. Fluctuations in term 1b, figure 17, and 2b, figure 18, also lends support to this possibility due to their fluctuations. Neither term 3 of figure 16 nor term 3b of figure 19 showed a large degree of fluctuation and neither of these terms were correlated with vertical velocity. Therefore, the above energetics were recalculated using a 120 day history record

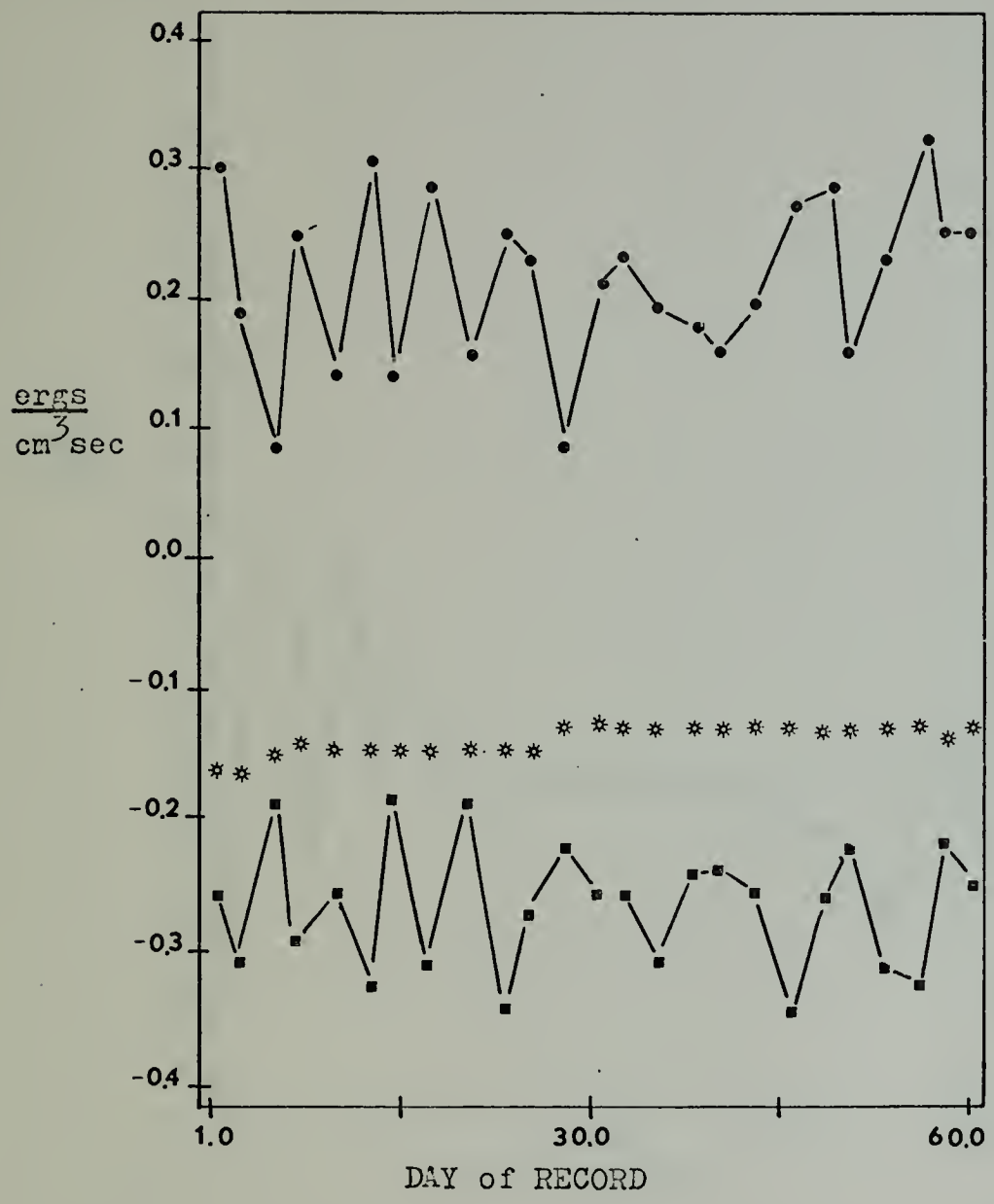

Figure 16. Contribution by Term1x10^5(•), Term2x10^6(▪), Term3x10^5(*), to the Balance of APE, Eq. (30).

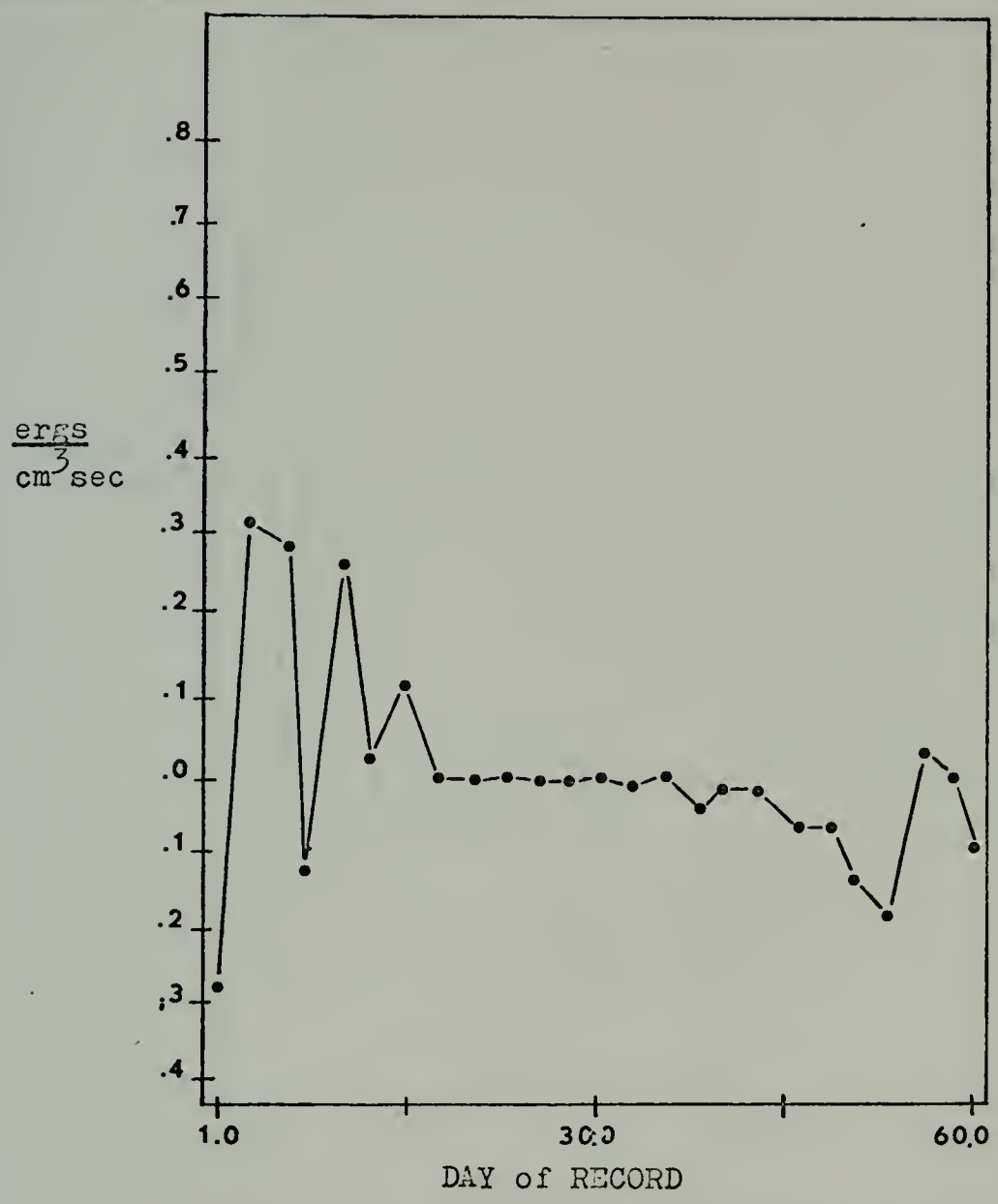

Figure 17. Contribution by Term1b x10^9 to the Balance of APE.

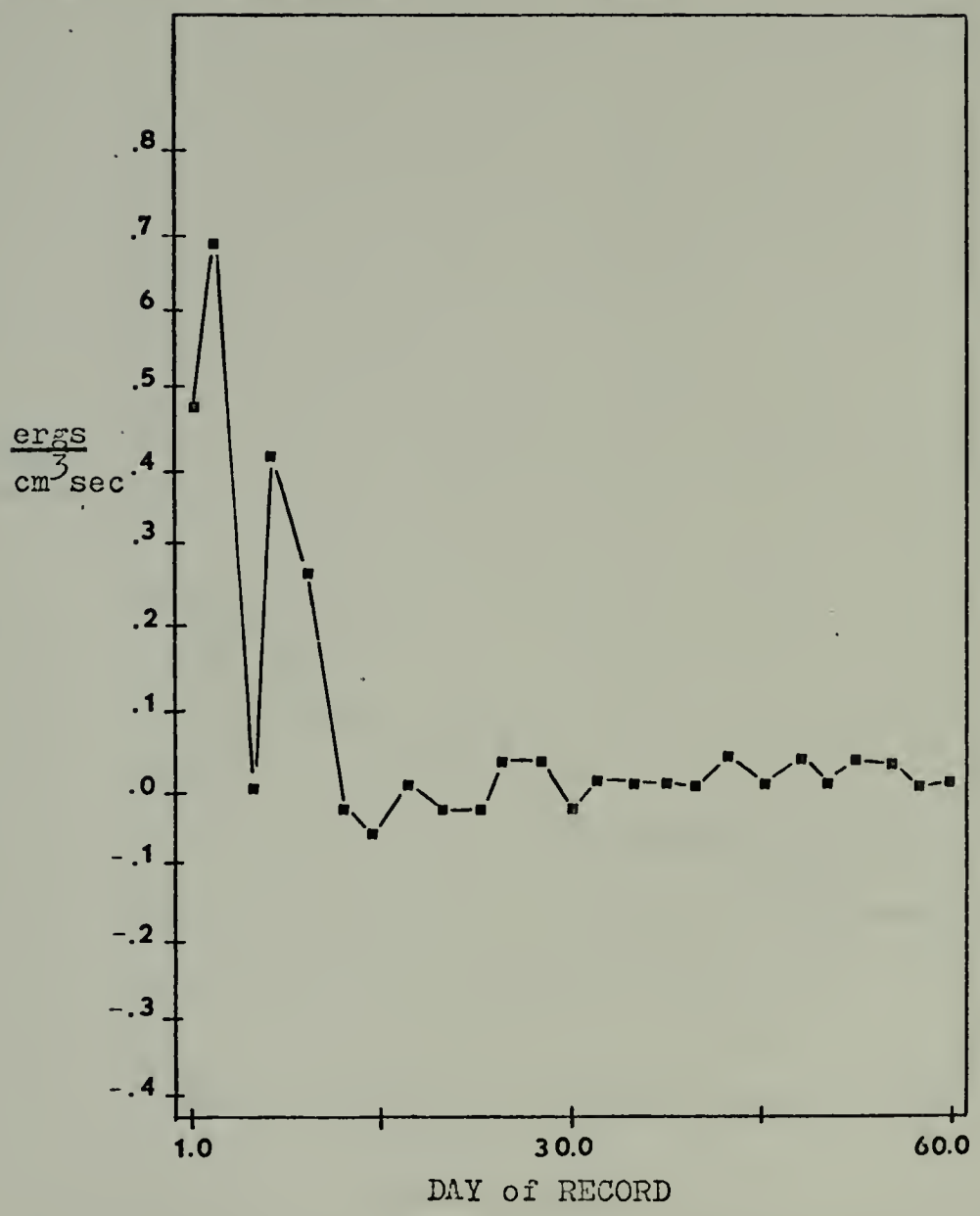

Figure 18. Contribution by Term2b $x10^{7}$ to the Balance of APE.

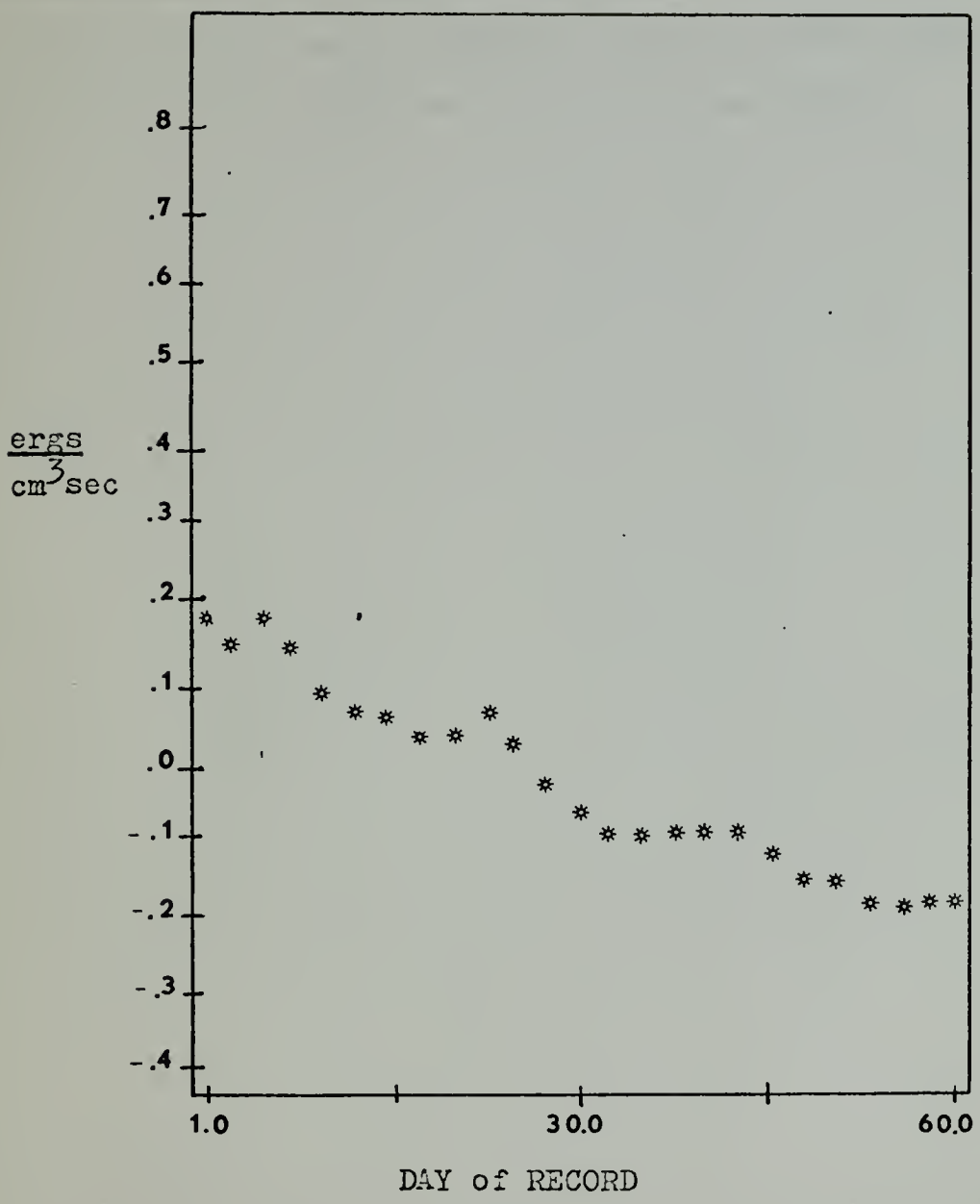

Figure 19. Contribution by Term3b $x10^5$ to the Balance of APE.

which began on day 10050 and ended on day 10170. No essential changes occurred in any of the terms except term 1b, which was still small, but negative for the 120 day average. Since a 120 day average would probable be more accurate than a 60 day average, the eddies were felt to be baroclinic.

VI. CONCLUSION

The results obtained from this study indicated that both the general circulation model and the MODE model were mechanically driven by the wind stress and not thermally driven to a great extent. The below diagram shows the transformation of energy from its generation by the wind stress to its dissipation through transient eddies as indicated by the results from the MODE model.

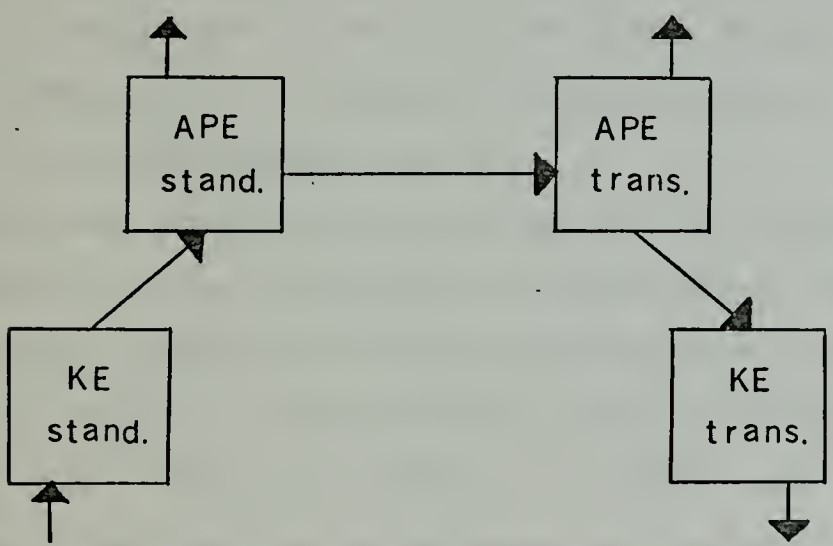

The atmospheric wind circulation acts on the ocean surface creating large scale standing motion. Some of the kinetic energy of the standing motion is transformed to standing available potential energy of the ocean. Approximately half of the input of energy to standing available potential energy is lost through non-convective heating by standing

motion. About one-fourth of standing available potential energy is transformed to transient available potential energy, where a large portion is lost through transient non-convective heating. A small portion, in the transient available potential energy balance, is transformed to kinetic energy of transient motion where it is lost through dissipation. Whether the transient available potential energy is the primary source for the transient kinetic energy must be determined by a study of the transient kinetic energy balance.

In the atmosphere, forcing is by the heating and the energy transformations are from available potential energy of standing motion to transient available potential energy, then to transient kinetic energy.

The main conclusion is that baroclinic instability is a possibility for maintaining the MODE eddies. The general circulation model showed energy transformations from eddy kinetic energy to eddy available potential energy for large-scale quasi-steady state motion. The MODE model showed the energy transformations to be opposite, from eddy available potential energy to eddy kinetic energy, for transient motion. Therefore, during periods of baroclinic instability, eddy available potential energy is aiding in the maintenance of the eddies.

LIST OF REFERENCES

1. Barrett, J.R., "Available Potential Energy of Gulf Stream Rings," Deep-Sea Research, v.18, p. 1221-1231, December 1971.

2. Haney, R.L., "A Numerical Study of the Response of an Idealized Ocean to Large-Scale Surface Heat and Momentum Flux," Journal so Physical Oceanography, v.4, No.2, p. 145-167, April 1974.

3. Lorenz, E.N., "Available Potential Energy and the Maintenance of the General Circulation," Tellus, v. 7, p. 157-167, May 1955.

4. Wright, W.R., "Northern Sources of Energy for the Deep Atlantic," Deep-Sea Research, v. 19, p. 865-877, December 1972.

INITIAL DISTRIBUTION LIST

		No. Copies
1.	Defense Documentation Center Cameron Station Alexandria, Virginia 22314	2
2.	Library (Code 0212) NPS Monterey, California 93940	2
3.	Prof. R.L. Haney Code 51 Hy	3
4.	M.E. Alcorn 1271 Spruance Rd. Monterey, California 93940	3
5.	Prof. G.J. Haltiner Code 51 Ha	1
6.	Meteorology Dept. Code 51 Library	1
7.	Naval Oceanographic Office Library (Code 3330) Washington, D.C. 20373	1
8.	Commander Naval Weather Service Command Naval Weather Service Headquarters Washington Navy Yard Washington, D.C. 20390	1
9.	Fleet Numerical Weather Central NPS Monterey, California 93940	1

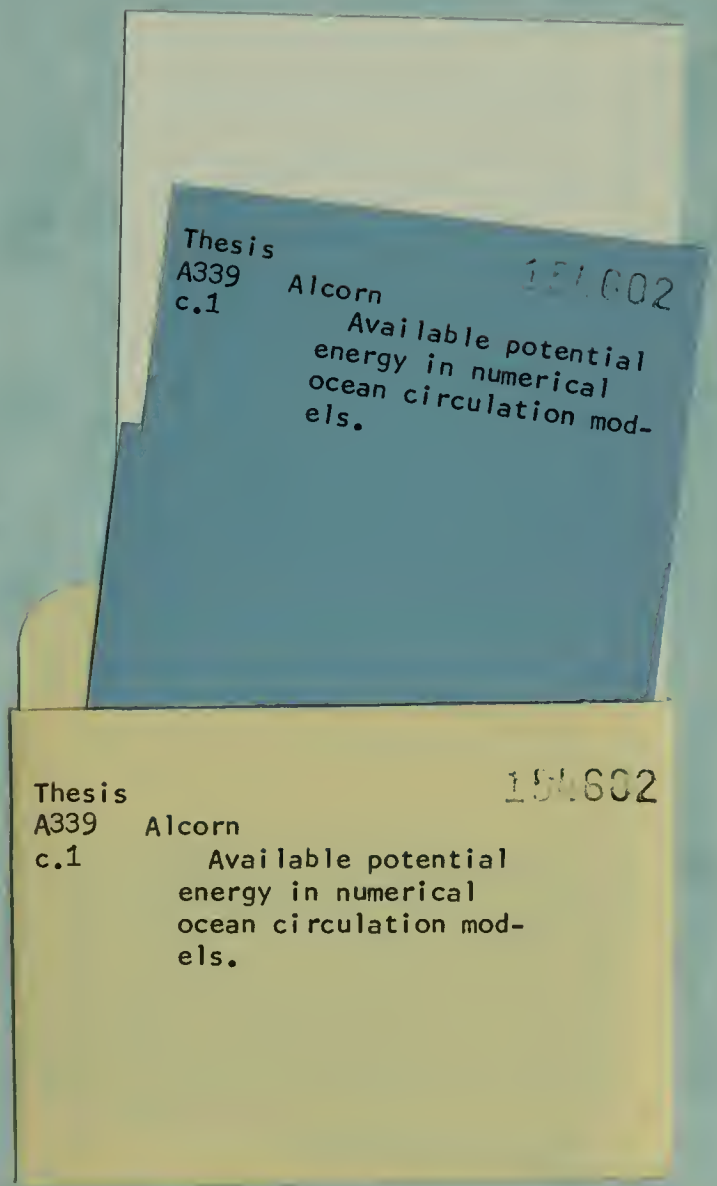

Thesis
A339 Alcorn
c.1 Available potential energy in numerical ocean circulation mod-
els.
151602